Laser-based displays: a review

Kishore V. Chellappan, Erdem Erden, and Hakan Urey*

Optical Microsystems Laboratory, Department of Electrical Engineering, Koç University, Istanbul, Turkey

*Corresponding author: hurey@ku.edu.tr

Received 11 January 2010; revised 9 June 2010; accepted 9 July 2010;
posted 13 July 2010 (Doc. ID 121708); published 4 August 2010

After the invention of lasers, in the past 50 years progress made in laser-based display technology has been very promising, with commercial products awaiting release to the mass market. Compact laser systems, such as edge-emitting diodes, vertical-cavity surface-emitting lasers, and optically pumped semiconductor lasers, are suitable candidates for laser-based displays. Laser speckle is an important concern, as it degrades image quality. Typically, one or multiple speckle reduction techniques are employed in laser displays to reduce speckle contrast. Likewise, laser safety issues need to be carefully evaluated in designing laser displays under different usage scenarios. Laser beam shaping using refractive and diffractive components is an integral part of laser displays, and the requirements depend on the source specifications, modulation technique, and the scanning method being employed in the display. A variety of laser-based displays have been reported, and many products such as pico projectors and laser televisions are commercially available already.

OCIS codes: 030.6140, 080.2175, 120.2040, 140.2010, 140.3298, 140.3300.

1. Introduction

Laser-based displays have been under active development over the past 50 years, but commercial viability of the technology was limited mainly due to the large size and high cost of laser sources. Recent developments in visible laser technology are expected to give momentum to the development of laser-based displays for the consumer market. Earlier laser projectors were inspired by the beam-scanning technology used in cathode ray tubes. The quest for miniaturization and high efficiency replaced the modulators and scanning technologies in these type of projectors with directly modulatable laser sources and scanning mirrors based on micro-electromechanical systems (MEMS) technology, respectively. Although diode laser technology could produce powerful blue and red lasers based on gallium nitride (GaN) and aluminum indium gallium phosphide (AlInGaP), respectively, a direct emitting green laser diode was not available until recently. Nichia Corporation and Osram Opto Semiconductors demonstrated 515 nm direct emitting laser diodes based on indium gallium nitride (InGaN), which is expected to replace less-efficient frequency doubled green lasers. One of the laser-based displays available on the market is "LaserVue," a laser rear-projection television from Mitsubishi. Other companies, such as Microvision, Alcatel-Lucent, Light Blue Optics (LBO), and Explay, are also developing their own laser display architectures for the mass market. Requirements on the source largely depend on the display architecture. For compact laser projectors for mobile devices, wall plug efficiency of the laser source is an important consideration. Although a laser-based display can offer a wide color gamut compared with other display technologies, it also comes with a problem specific to laser light, the speckle, which results from the coherence of laser light.

This review is on display technologies with lasers as light sources but excludes laser shows, which display only a low amount of information. Section 2 deals with different laser technologies available and considers the advantages and disadvantages of each technology as well as discusses potential technologies. Sections on display white balancing (Section 3) and laser safety (Section 4) are included before the discussion on speckle in Section 5. In Section 6, different beam-shaping techniques are discussed,

0003-6935/10/250F79-20$15.00/0

and, finally, in Section 7, laser-based display systems are reviewed.

2. Lasers and Requirements for Displays

Even though the idea of using lasers for displays was proposed in the 1960s [1], it is the availability of lasers emitting red, green, and blue colors that triggered the recent development of portable laser projectors. An immediate advantage of using spectrally pure laser light for displays is the wide color gamut it can produce. Although gas lasers are available with a wide range of wavelengths, being bulky and less efficient makes them unsuitable for the mass production display market. Moreover, they require external modulators, which increase the cost and complexity of the system. An example system is the laser projector reported by Kim *et al.*, which used a Kr–Ar laser system with beam scanning [2]. Requirements of the laser source depend on the architecture of the display. For a flat panel backlit display, the laser beam M^2 parameter can be a few hundred times larger than that of a diffraction limited beam [3]. Display systems based on the flying spot approach are considered to be more suitable for mobile devices [4]. Such an approach requires that the laser beam be collimated while maintaining the small beam size, which places restrictions on the selection of the source. As a TEM_{00} laser beam can be considered as a true point source, such a beam is the ideal choice of the designer in this case. It is claimed that a fast moving spot can be perceived about 30% smaller compared to a static spot, thereby increasing the line resolution [5]. In the following sections, the state of the art in laser systems, such as edge-emitting laser diodes, diode-pumped solid-state lasers, vertical-cavity surface-emitting lasers (VCSELs), and optically pumped semiconductor lasers (OPSLs), is reviewed.

A. Edge-Emitting Laser Diodes

In 1962, the first semiconductor laser based on GaAs was invented independently by Hall *et al.*, Nathan *et al.*, and Quist *et al.* [6–8]. These devices required cryogenic temperatures, and they were operated in the pulsed mode. Continuous wave (CW) operation at room temperature was later demonstrated by Alferov *et al.* and Hayashi *et al.* with a heterojunction approach, which gave rise to an efficient confinement of carriers and photons to the active region of the device [9,10]. Later, the introduction of fiber optic communication systems proved that the invention of the semiconductor laser was one of the revolutionary steps in the history of lasers.

Semiconductor diodes emitting in the visible region are made of GaInN/GaN and AlGaInP/GaAs [11]. Direct emission green lasers were not available, but recently Nichia Corporation reported devices based on InGaN, which emits at 515 nm. Osram, Incorporated, also reported their InGaN-based 50 mW green laser which operates at 515 nm. LaserVue, the recent laser television product from Mitsubishi, uses red and blue edge-emitting diodes based on modified AlGaInP and GaN material systems [12]. The structure of an edge-emitting diode laser is shown schematically in Fig. 1.

Despite having the advantage of being directly modulatable, the output wavelength of this type of lasers can vary with the junction temperature, which will in turn adversely affect the color balance of the display, if left uncontrolled. For a red laser diode, the deviations from the specified wavelength should be less than 0.5 nm, whereas power variations should be kept below 0.7%. Temperature stabilization can be done with the help of thermoelectric cooling devices [13]. Other disadvantages of lasers with this architecture are the limited output power and the highly astigmatic beam. In order to obtain high power, an array of diodes is often used. Although higher power can be obtained from such an array, the fill factor is much less compared to single emitters, and special techniques are required for producing uniform illumination and for fiber coupling [14]. Also, because of the mismatch in the coefficient of thermal expansion of different layers of a diode laser array and that between the laser bar and its heat sink, the individual emitters may not appear on a line while in operation. This artifact is called the "smile" and produces a nonlinear array of emitters, which makes beam shaping and fiber coupling a difficult task [15]. In order to correct wavefront errors caused by defocus, aberrations, and misalignment of the source and lens, corrector phase plates can be used [16]. More about beam shaping is discussed in Section 6. Despite having these drawbacks, using an array of emitters has the advantage of reduced speckle contrast in the display by a factor of $1/\sqrt{M}$, where M is the number of uncorrelated speckle patterns generated by the emitters [17]. The speckle issue is discussed in Section 5. The article by Endriz *et al.* describes different high-power laser arrays and the operating parameters in detail [18].

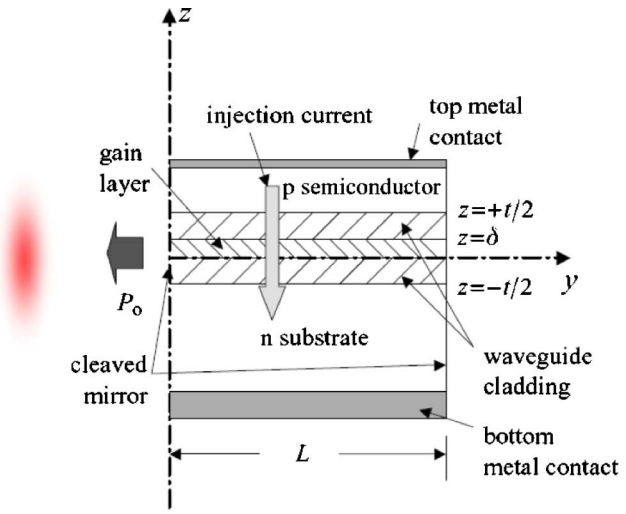

Fig. 1. (Color online) Structure of an edge-emitting diode laser and its output intensity distribution (taken from Ref. [168]).

B. Diode-Pumped Solid-State Lasers

Diode-pumped lasers are capable of generating watts of optical power at the primary wavelengths of interest through nonlinear frequency conversion processes. The red-green-blue (RGB) laser system reported by Hollemann *et al.* used such an approach to produce an RGB combined optical power of 18 W [19]. Another system by Nebel and Wallenstein demonstrated the generation of laser light with output powers of up to 7.1 W at 629 nm, 6.9 W at 532 nm, and 5.0 W at 446 nm. The white output power was 19 W, produced with 110 W of optical pumping with diode lasers [20]. But these kinds of systems are costly and require complicated optical setups for the frequency conversion processes. As there was no direct emitting green semiconductor lasers, most of the display products use the frequency doubling of infrared light for producing green. The Corning Green Laser G-1000 module uses a distributed Bragg reflector laser operating at 1060 nm [21] followed by frequency doubling in a periodically poled lithium niobate waveguide [22]. Figure 2 illustrates the operation of this laser unit. The entire unit can be enclosed in a volume of 0.69 cc. The small form factor and high optical power output make this laser suitable for small projectors.

The green light source in Mitsubishi's laser television is a 15 emitter array of lasers emitting frequency doubled 532 nm light. In the air-cooled version, this module, with a volume of 5 cc, could generate ≈3.8 W of green light [12]. There are many reports in the literature that demonstrate generation of the primary colors based on nonlinear optical frequency conversion processes [23,24]. Recently an RGB laser source was demonstrated based on frequency conversion in a single lithium tantalate crystal [14]. The Evans & Sutherland Laser Projector (ESLP) uses laser systems that employ a nonlinear frequency conversion processes to produce the primaries at 631, 532, and 448 nm [25].

C. Vertical-Cavity Surface-Emitting Lasers

Display applications sometimes require high output optical power and good beam quality, but conventional semiconductors are unable to meet both needs at the same time. VCSELs use a surface-emitting structure, in contrast to the edge-emitting conventional diodes, giving better beam quality. The first of this type of diodes was introduced by Soda *et al.* in 1979 [26]. The beam is circular, but here also, the output power is limited and stacking of diodes is necessary to produce high optical powers. Figure 3 shows the typical architecture of surface-emitting laser diodes. An advantage of VCSELs is that, unlike edge-emitters, they can be fabricated as monolithic arrays, eliminating the need for single high-powered lasers and allowing for parallelism in drawing the image [27].

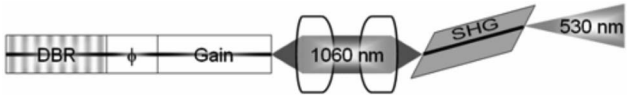

Fig. 2. Operation of the G-1000 laser from Corning. Taken from Ref. [22], Copyright 2008 Society for Information Display.

Firecomms, Limited, produce low-power (≈1 mW) red VCSELs with an AlGaInP active region, which emit in the 650–690 nm region [28]. But the use of this wavelength region is not preferred for displays, as the human eye is less responsive here, requiring higher optical power from the red for effective white balancing of the display. More about color balancing is discussed in Section 3.

Necsel demonstrated high-power RGB laser arrays of extended cavity surface-emitting lasers. This special laser structure called the Novalux Extended Cavity Surface-Emitting Laser (NECSEL) uses intracavity frequency doubling of infrared light from VCSELs with an InGaAs active region to produce visible light at 615, 532, and 465 nm [29]. Each single emitter of the array could generate a power of more than 100 mW. One of the advantages is that, although the efficiency can vary, the output wavelength of this laser system is not temperature sensitive, as a volume Bragg grating is used as the output coupler. Figure 4 shows the RGB units of these lasers. The green and blue units generate 3 W, while the red unit emits more than 4 W.

D. Optically Pumped Semiconductor Lasers

This class of lasers is said to deliver high optical power with good beam quality. In contrast to VCSELs, where electrical current is used for triggering and maintaining lasing, here optical pumping is used to trigger and maintain it. A small drawback is that the external cavity of this type of laser requires alignment. But the high power and good beam quality make them attractive for display applications.

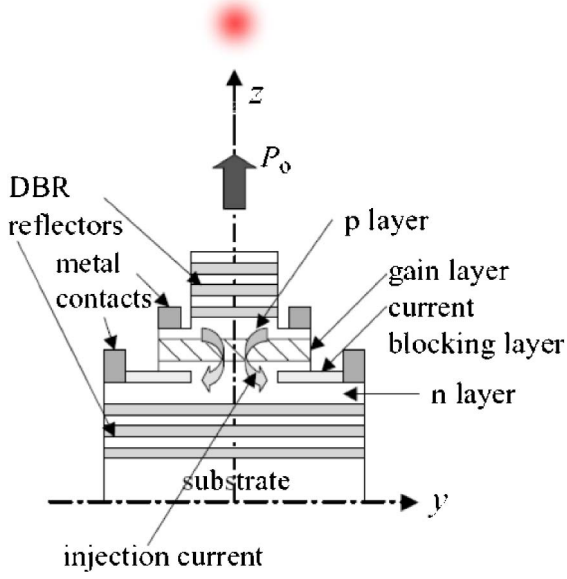

Fig. 3. (Color online) Structure of a VCSEL and its output intensity distribution. Taken from Ref. [168].

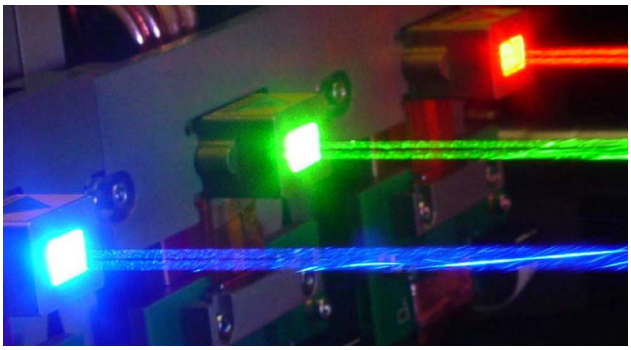

Fig. 4. (Color online) NECSEL arrays in operation. Photo courtesy of Necsel Intellectual Property, Incorporated

Figure 5 shows the structure of an OPSL employing the side-pumping scheme.

The importance of this technology is the possibility of producing high power with good beam quality and the proposed scalability [30]. More than 8 W of optical power was produced at 1000 nm with an M^2 value of <1.8 by Lutgen *et al.* [31]. Kim *et al.* demonstrated 2.7 W green and 1.4 W blue lasers with good beam quality using an end-pumping scheme in order to improve pumping efficiency [32]. The Genesis series of high-power lasers from Coherent, Incorporated, uses the OPSL technology to produce wavelengths at 639, 532, 577, 480, and 460 nm with power levels ranging from 500 to 8000 mW. Osram employed optical pumping to produce efficient and compact green lasers with powers up to 50 mW [33]. They also built red-green minimodules of these lasers, which demonstrates the scalability of the technology [34]. The electrical-to-optical power conversion efficiency was 10%–20% with power outputs of 50–100 mW for green and 150–300 mW for red. A review of this class of lasers, which are also called semiconductor disk lasers, may be found in Refs. [35,36].

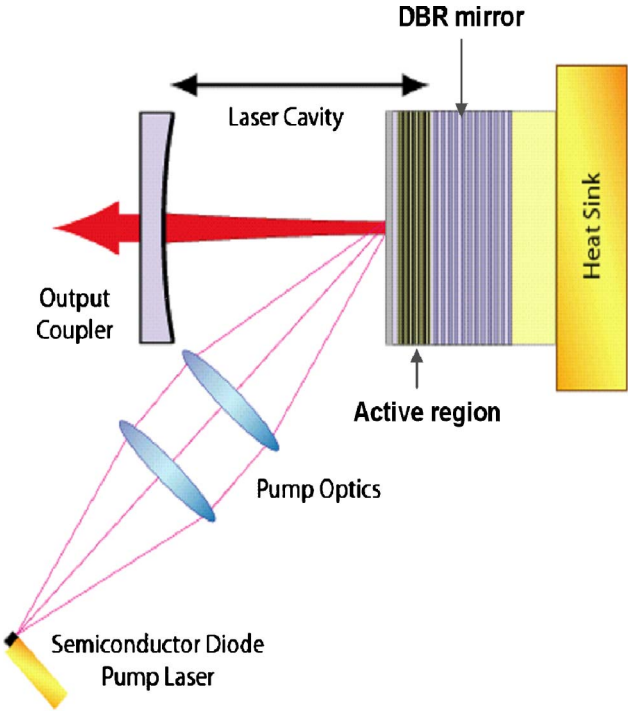

Fig. 5. (Color online) Schematic of an OPSL, reproduced with permission from Ref. [30].

3. White Balancing and Throughput Evaluation

Attempts to understand the science of color dates back to the time of Isaac Newton, who successfully dispersed and recombined white light with the help of prisms [37]. An important advantage of laser-based displays is the wide range of colors they can offer to the viewer. No other display type is capable of producing the color gamut offered by a laser display with three primaries, which can be more than 80% of the total range of colors perceivable by humans [38,39]. The cone photoreceptors of the eye, responsible for bright light viewing conditions (photopic vision), are mainly sensitive to the red, green, and blue regions of the visible spectrum [40,41]. Selecting the wavelengths of the primaries for additive mixing and the required optical powers depends on the response of the human visual system at the respective wavelengths.

A preliminary set of color matching functions, which form the basis of colorimetry, were derived from the color matching experiments by W. D. Wright and J. Guild. Later in 1931, Commission Internationale de l'Éclairage (CIE) derived a set of new color matching functions $(\bar{x},\bar{y},\bar{z})$ from the original experimental results in order to avoid negative values of the coordinates [41]. The procedures adopted were also discussed in the literature [42]. The CIE1931 XYZ color matching functions are shown in Fig. 6, which are calculated from the original experimental values.

The chromaticity diagram with the color coordinates or the chromaticity coordinates, which depend only on the hue and saturation, is shown in Fig. 7. The monochromatic wavelengths are located at the outer border of the chromaticity diagram. The

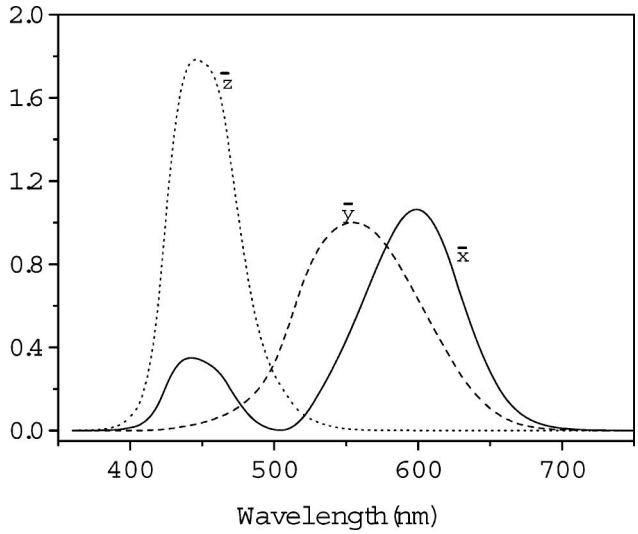

Fig. 6. 1931 CIE XYZ color matching functions of the standard observer.

diagram represents the color gamut of the human visual system.

For displays, relative luminance of the primaries are decided based on the display white point. ITU-R BT.709 designated coordinates of the white point are (0.3127,0.3291). It is possible to determine the relative optical powers required for this white point if the color coordinates of the primaries are known [43]. Alternatively, the required optical power of three primaries with specified wavelengths $R(\lambda 1)$, $G(\lambda 2)$, and $B(\lambda 3)$ for a specified color temperature can be evaluated if the tristimulus values X and Z are known (Y is normalized to 100). The following matrix operation can be performed to evaluate the required optical power:

$$\begin{bmatrix} \bar{x}(\lambda_1) & \bar{x}(\lambda_2) & \bar{x}(\lambda_3) \\ \bar{y}(\lambda_1) & \bar{y}(\lambda_2) & \bar{y}(\lambda_3) \\ \bar{z}(\lambda_1) & \bar{z}(\lambda_2) & \bar{z}(\lambda_3) \end{bmatrix}^{-1} \begin{bmatrix} X \\ Y \\ Z \end{bmatrix} = k \begin{bmatrix} P(\lambda 1) \\ P(\lambda 3) \\ P(\lambda 3) \end{bmatrix}. \quad (1)$$

For example, for a color temperature of 6500 K (daylight), denoted as D65, the XYZ coordinates are $X = 95.017$, $Y = 100.000$, and $Z = 108.813$. If one tries to obtain 6500 K white light from three laser wavelengths, the optical power ratio depends on the wavelengths chosen. As shown in Table 1, as the red wavelength approaches 700 nm, the power required from red goes up.

A display system produced with these wavelengths will be able to reproduce the colors enclosed in the triangular region obtained by connecting these primary wavelengths in the chromaticity diagram. It can be immediately seen that displays with three primaries are unable to reproduce all colors perceivable

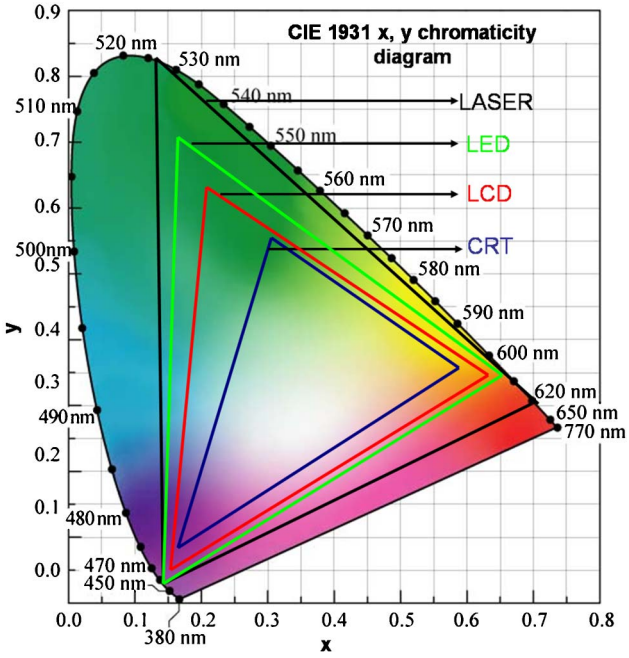

Fig. 7. (Color online) 1931 CIE xyY chromaticity diagram. The color gamut possible with CRT, LCD, LED, and laser-based displays is shown.

Table 1. Laser Optical Power Ratio for 6500 K at Some Representative Laser Wavelengths (in nm)

Red	Green	Blue	Power Ratio (R:G:B)
633	532	465	1:0.73:0.64
635	532	465	1:0.68:0.60
640	532	442	1:0.66:0.46
650	532	442	1:0.42:0.29
670	532	442	1:0.13:0.09

by the human visual system. Instead of using three primary wavelengths, one can use four or more primary wavelengths for an enhanced color gamut at the expense of increased design complexity and cost. The methods for achieving a desired white point in these multiprimary displays are well described in the literature [43–47].

The lumen output of the projector is directly related to the power output from the light source. Power budgeting of the display can be done if the transmittance of the optical components at the respective wavelengths are known. But a complete and accurate estimation of the brightness require a model that takes into account the étendue of the components and the light source [48]. The étendue of a source is a function of the emitting area of the source orthogonal to the axis of propagation of light and the solid angle subtended by the cone of light at that point. This is an invariant quantity and is often expressed as the optical invariant or the Lagrange invariant. As lasers are sources with the lowest étendue, optical systems made with them are more likely to be not étendue limited. The étendue limitation comes mainly from the modulators and components with low étendue, such as apertures or stops in the optical train [49]. Another important parameter is the contrast of the display, which can also be modeled by taking into consideration factors such as diffraction, scattered light, and ghost images [50]. Other parameters, such as the modulation transfer function and resolution of laser scanning systems, have also been discussed in the literature [51].

4. Laser Safety

Laser radiation falls in the category of nonionizing radiation, unlike x rays and gamma rays. Although there are other risks, such as chemical, electrical, and other secondary hazards associated with a laser unit, the mostly discussed risks are eye and skin hazards caused by laser radiation. A laser with sufficient optical power can cause corneal and retinal burns or cataracts, depending on the level of exposure. Skin burns are also likely at high powers with the possibility of skin carcinogenesis, if the exposure is at certain ultraviolet wavelengths [52]. In laser-based displays, only wavelengths in the range from 400 to 700 nm are used. But there may be spurious emission of infrared or ultraviolet if the technology used for the generation of the primaries utilize nonlinear optical processes, such as second harmonic generation or sum/difference frequency generation.

But these can be effectively removed with appropriate filters.

As can be seen in Fig. 8, the biological matter that precedes the retina has good transmission in the 400–1400 nm spectral region. This range of wavelengths is called the retinal hazard region [53], as it will reach the retina with an irradiance that is 10^5 times greater than the corneal irradiance owing to the focusing action of the lens [52]. All other wavelengths are absorbed at the exterior parts of the eye, such as the cornea and the lens, with possible damage to these parts if the optical power is high. Near the blue end of the spectrum, retinal damages are photochemical in nature, while at the red end, thermal damage dominates. It was pointed out that not all alleged "laser eye injuries" are laser injuries; some of them could even be self-inflicted [54,55].

Based on the wavelength and optical power of emission or, more precisely, the hazard potential, lasers are classified and control measures are specified by safety standards such as the American National Standards Institute (ANSI) Z136.1-2007 American National Standard for Safe Use of Lasers, guidelines of the International Commission on Nonionizing Radiation Protection (ICNIRP), and the International Electrotechnical Commission (IEC) standard IEC60825-1:2007. In order to evaluate the hazard potential of a laser-based display system, one has to determine the maximum possible exposure under a worst-case scenario [56]. If the evaluated exposures are below the maximum permissible exposure (MPE) for laser radiation laid out by the above-mentioned standards, the display may be considered eye safe. The MPE may be considered as exposure levels to which one can be exposed without suffering adverse eye or skin injuries. The ICNIRP uses the term exposure limit (EL), ANSI and IEC use MPE, and the American Conference of Governmental Industrial Hygienists (ACGIH) uses threshold limit value; all have the same limiting values [56].

A. Exposure Limits

Lasers are classified into seven different classes, namely, Class 1, 1M, 2, 2M, 3R, 3B, and 4 in IEC 60825-1, of which Class 1 and 1M are considered safe for long-term intentional viewing. Other classes have an associated safe exposure duration; for example, Class 2 is eye safe for accidental viewing up to 0.25 s. This classification is based on a quantity called the accessible emission limit (AEL), which is the product of the MPE for a specified duration of exposure and the area of the collecting aperture. This aperture area is normally taken as $\sim 0.39\,\mathrm{cm}^2$, corresponding to the dark-adapted, maximal, dilated eye pupil diameter of 7 mm. If the estimated accessible emission is within the specified limits for a particular class of laser, then the laser system or display device belongs to that class. When calculating MPEs, one has to make a distinction between pulsed and CW lasers. For pulsed lasers, the peak power (energy per pulse duration) can be very high, while the average power (energy/second) is low. From 100 fs to 18 μs, three different MPE values are specified based on the exposure duration [56]. If the exposure is above 18 μs but less than 10 s, the MPE is a function of exposure time (t) and is given by $18C_E t^{0.75}\,\mathrm{J/m^2}$. For continuous viewing ($t = T_2$ s to 30,000 s), the MPE is given by $18C_E T_2^{-0.25}\,\mathrm{W/m^2}$ (Table 4 of Ref. [56]). C_E is a correction factor, which is unity for sources which subtend an angle of less than 1.5 mrad at the eyes of the viewer at a distance of 100 mm.

In some cases, the beam directly scans the eyes of the viewer; examples are laser shows and the inadvertent view of the direct output from a laser projector. The eye pupillary, blink, and aversion responses limit the unintentional exposure to 0.25 s in these circumstances. For such a scenario, the exposure is repetitive or there may be multiple pulses within one exposure duration. Here three rules apply [56]:

- The exposure from any single pulse in a series of pulses should not exceed the MPE for a single pulse of that duration.
- The exposure from any group of pulses delivered in time T should not exceed the MPE for time T.
- The exposure from any single pulse in a series of pulses should not exceed the MPE for a single pulse multiplied by $N^{-0.25}$, where N is the number of pulses.

It was proposed that if the scan rate is increased sufficiently high such that the pulse duration is less than 18 μs, the hazard factor will reduce as the MPE starts to change inversely with the exposure time [57]. For a scanned CW laser beam (400–700 nm), the MPE expression may be written as

$$\mathrm{MPE}_{\text{single pulse}} = N^{-0.25} \times 18 \times t^{-0.25}\,\mathrm{W/m^2}, \qquad (2)$$

where N is the number of pulses, each having a duration of t seconds. It has to be noted that irradiance for hazard evaluation purposes are estimated assuming the laser power is distributed over a circular aperture of diameter 7 mm, even if the beam diameter is less than 7 mm. Inadvertent viewing of the direct

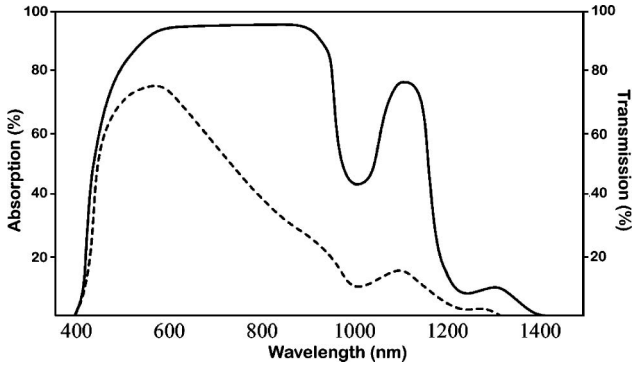

Fig. 8. Transmission spectrum of the eye from the cornea to the retina (solid curve) and absorption of the retinal pigment epithelium as a function of wavelength (dotted curve). From Ref. [61], with kind permission of Springer Science+Business Media.

output from a laser projector can damage the eyes of the viewer. Instead of turning off the lasers and annoying the entire audience, control circuits for selectively turning off the obstructed region of the projected image can be implemented [58]. For handheld scanned beam laser projectors that are emerging, the worst-case scenario can be any one of the following depending on the configuration: (i) the eye is at 100 mm and relaxed (focused at infinity) and (ii) the eye is focused at the exit lens or the scan mirror from a distance of 100 mm. If the scan speed is sufficiently high so that the scan duration is less than the thermal confinement time of 18 μs, the image on the retina can be considered as a line that allows an increase in the AEL due to the increased angular subtense (α) and condition (ii) becomes the worst case [59]. Typical 10 lm projectors are identified as Class 1 or Class 2 based on their configuration. A recent study showed that the output from many lamp-based commercial projectors are capable of producing eye hazards equivalent to that of Class 2 laser products [60].

B. Safety Filters

The aversion response of the eye is usually taken into account when evaluating eye safety factors. It is always recommended to wear safety filters with sufficient optical density (OD) while working with high-power lasers. The following equation can be used for the estimation of the OD required for a specific wavelength [52]:

$$\mathrm{OD}(\lambda) = \log_{10} \frac{H_0}{\mathrm{MPE}}, \tag{3}$$

where H_0 is the expected worst-case exposure, with units identical to that of the MPE. For example, for a 6 W (CW) 640 nm laser, assuming a worst-case condition of intrabeam viewing, $H_0 = 6(\pi 0.0035^2) = 155,986\ \mathrm{W/m^2}$. As the MPE is $10\ \mathrm{W/m^2}$ at this wavelength, this laser requires a filter with an OD of 4.2. For more comprehensive discussions on laser safety, Refs. [61,59] may be referred to.

5. Speckle in Laser Displays

When an object is illuminated with a coherent light source, such as a laser, the scattered light has components with different delays, which are caused by the roughness of the illuminated surface. As the scattered light propagates further, these coherent but dephased components interfere and produce a granular intensity pattern called speckle on the screen [17]. Speckle formation in free space and in imaging systems is shown schematically in Fig. 9. The shape and the linear dimensions of the speckle pattern are governed by the roughness and the curvature of the object surface [62]. The observed speckle pattern has a dependence on the spatial location of the eyes of the viewer as well as the resolution of the visual system.

The pattern consists of bright spots created by constructive interference, dark spots created by destructive interference, and areas with intermediate brightness levels. Although speckle formation can be beneficial in the precise measurement of displacements or image reconstruction [63], it is an undesired effect in laser-based display systems, as it destroys the information content and reduces the resolution [64]. It is estimated that the human visual system can detect speckles with a contrast value down to 4% [65].

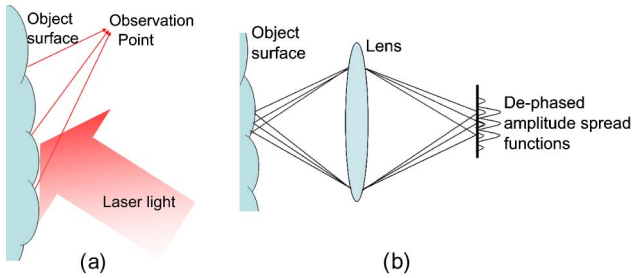

Fig. 9. (Color online) Speckle formation in (a) free space and (b) an imaging system.

An example of the effect of speckle on images produced by laser projection displays and the effect of a commercial speckle reduction module are shown in Fig. 10. Speckle is easily observed while viewing laser-illuminated objects, and it can be observed even with femtosecond lasers but with lower speckle contrasts [66]. Speckle and its characteristics are widely studied in the literature owing to the interesting characteristics of speckle [67,68]. If a laser-illuminated object moves, a corresponding change in the local speckle contrast is observed, which can provide information about the movement of the object. Speckle contrast variations can be utilized in optical displacement sensors [69,70] and blood flow measurements [71]. In order to reduce speckle, many different methods have been suggested [72].

A. Techniques for Speckle Reduction

Speckle is quantified in terms of speckle contrast, which is defined as the ratio of the standard deviation of the intensity fluctuation to the mean intensity. It was shown that addition of M uncorrelated and noninterfering speckle patterns on an irradiance basis reduces the speckle contrast by $1/\sqrt{M}$ [17]. In order to generate uncorrelated speckle patterns in

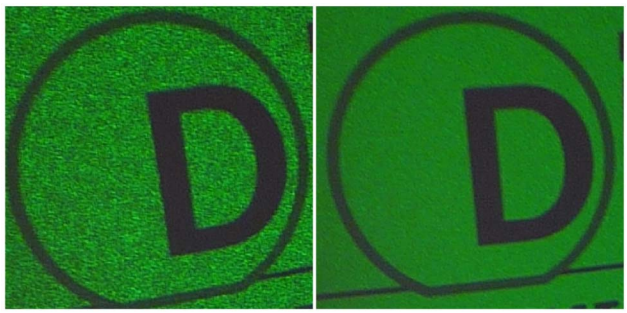

Fig. 10. (Color online) Effect of speckle reduction. Images produced by a monochrome DLP engine without (left) and with (right) Dyoptyka speckle reduction technology. Image courtesy Dyoptyka.

the spatial dimension, incident angle, wavelength, or polarization of the light source can be altered. Uncorrelated patterns in the temporal dimension can be created by placing and moving a scattering surface into the light path. The moving scattering surface creates a time-varying speckle pattern, and if the movement is fast enough, the speckle will be averaged out by the human eye.

Angular diversity for speckle reduction can be achieved with MEMS scanning devices working at 2–10 kHz that generate different illumination angles. Each angle of illumination provides a particular speckle image, and the contrast can be reduced to half of its initial value by averaging different speckle images within the exposure time of the sensor (e.g., within 1/60 s for the human eye) [73].

Using a broadband source reduces the temporal coherence and, therefore, can effectively reduce speckle without causing optical loss or design complexity. However, driving multiple laser diodes individually with different wavelengths is a very complex and costly task and is not useful for a laser-based television or projector system. In order to overcome this problem, a new laser diode array structure that exhibits self-induced spectrum widening has been suggested [74]. In this method, spectrum widening is achieved by controlling the thermal cross talk between adjacent emitters in a laser diode array. A laser projection display with a low speckle contrast of 2% is built by using the controlled laser diode array and a diffusion film. The diffusion film is located within the screen layers and makes oscillating movement with the help of a stepper motor. Figure 11 shows moving screen set ups for the front and back projection displays [74].

If the observer is close to the screen in a projection system, the perceived diameter of the speckle is typically small, and speckle can be reduced by reducing the temporal or the spatial coherence of the laser. In the far field, on the other hand, the average size of the speckles appears larger to the observers eyes; therefore, small phase changes are not sufficient to eliminate the speckle in the far field [65]. In order to remove speckle in the far field, boiling speckle patterns can be produced by using a diffractive optical element (DOE). A DOE is used to modulate the spatial phase and the amplitude of the unfocused scanning laser beam across its diameter. As can be seen in Fig. 12, as the unfocused laser beam passes through the DOE, it is split into a number of independent beamlets with a smaller diameter, which are partially focused on the screen with random phase distributions.

In the proposed system, beamlets illuminate different areas within one pixel on the screen and create multiple overlapping speckle patterns in the eyes of the observer. Then the speckle patterns are moved by rotating the DOE or by scanning the beamlets over the screen. The beamlets illuminate small moving areas on the screen as they move, and because of the roughness of the surface, a boiling speckle pattern is formed by the movement of these areas on the screen. The speckle is reduced as the boiling speckle pattern is averaged by the eye of the viewer.

Instead of moving a diffuser or the screen, a time-varying speckle pattern can be created using colloidal dispersion filled projection screens [75]. When the laser beam enters the screen, it scatters from the scattering globules inside the colloidal dispersion. A time-varying speckle pattern is formed by the scattered light, and this temporal averaging lowered the speckle contrast to 3%. The problem of blurring caused by the screen is reduced to acceptable levels by using highly scattering colloidal dispersion with highly forward-peaked scattering. This screen can be used with both single-emitter and multiemitter lasers and can bring additional reductions to the speckle contrast if it is combined with other methods.

Another method for creating a time-varying speckle pattern is using a dynamic polymer-based diffraction grating [76]. In this approach, diffracted light coming from the grating is used as the illumination source after collection and homogenization. A time-varying speckle pattern is created by the time-varying phase of the diffraction grating and

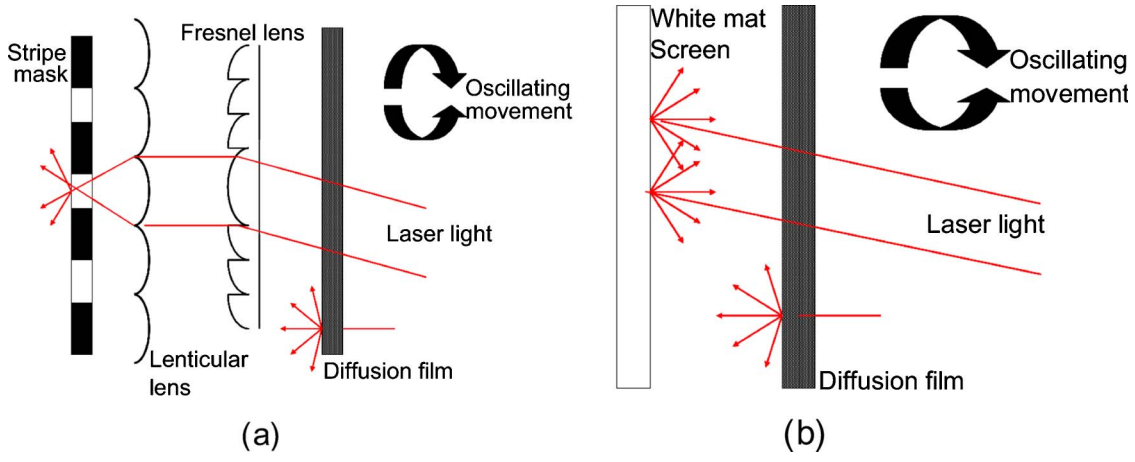

Fig. 11. (Color online) Moving screen in (a) rear projection and (b) front projection displays, from Ref. [74].

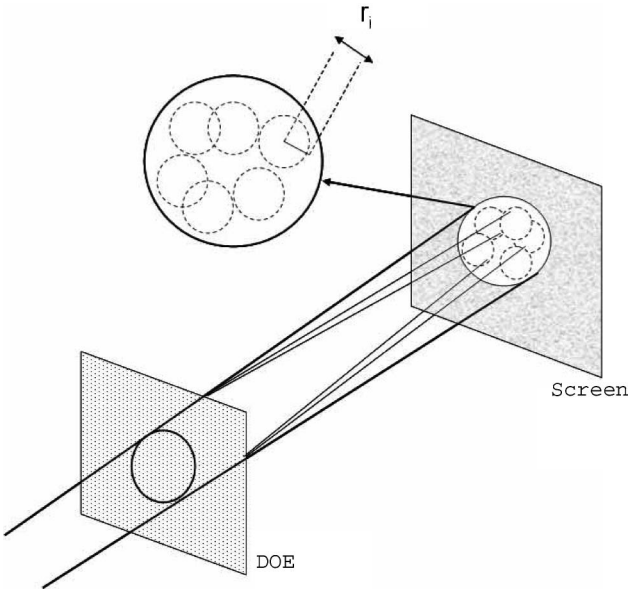

Fig. 12. Formation of independent beamlets with DOE, from Ref. [65].

subsequently averaged by a CCD camera with appropriate integration time.

Diffraction gratings can also be used as exit pupil expanders in scanning laser display systems. The DOE is placed at an intermediate image plane and expands the beam divergence angle by creating a large array of replicated exit pupils. In order to achieve good uniformity at the exit pupil, the DOE repeated cell size and the laser spot size should be comparable. If the laser spot is smaller than one DOE cell size, then a position-dependent random speckle pattern is observed. The design and the diffraction-order uniformity of binary diffraction gratings used for exit pupil expansion are discussed in the literature [77].

Although the stated speckle reduction techniques reduce the speckle contrast in considerable amounts, they do not completely remove the speckle noise and hot spot speckles remain [78]. The remaining hot spot speckles can be removed by implementing both a rotating diffuser and a running screen. This method was first applied in a monochrome laser projection system, which resulted in a speckle contrast of only 1.6%. The technique was successfully implemented in a commercial laser projection display (Fig. 13), where the image was formed by a digital light processing (DLP) system using a high-power RGB laser source and a 70 in. screen with a piezoelectric motor.

All the methods discussed so far reduce the speckle contrast by destroying the coherence with moving parts but also reduce the brightness by inserting additional components. Alternatively, speckle contrast values down to 3.5% can be achieved by using a nonmodal, spatially incoherent beam coming from a broad-area VCSEL source [79]. The source is driven with specific current values and illuminates a polarization scrambling screen. Visible lasers, which have low spatial coherence in the far field when working in the nonmodal regime, are required to implement this approach in laser projection applications.

Instead of using general speckle reduction techniques separately, it is better to find ways of combining them together and get even lower speckle contrasts. An example of this approach is the laser projector reported by Trisnadi *et al.*, in which speckle was reduced by creating angle, polarization, and wavelength diversities [80]. Angle diversity is achieved using a time-varying Hadamard diffuser that is placed in an intermediate image plane. When the light passes through the diffuser, the amplitude image is superimposed with the pure phase pattern of the diffuser. Because the intensity of the image does not change with phase modulation, the detected image on the detector is not affected. The diffuser divides each detector resolution spot into N smaller phase cells and assigns a phase to each cell, as shown in Fig. 14. Speckle is reduced as the spatial coherence among the phase cells in the resolution spot is destroyed.

In order to have polarization diversity, a polarizing beam splitter and a few centimeters of optical delay are used and orthogonal polarization states are created. The speckle patterns from two beams with different wavelengths become uncorrelated if the average relative phase shift created by the surface is $\approx 2\pi$ or more. A screen with near unity gain and a high degree of depolarization is used to create the required relative phase shift. When all these adjustments are applied to a grating light valve (GLV) laser projection system, shown in Fig. 15, the speckle is reduced from 70% contrast to 8% contrast for a single wavelength (532 nm).

It can be seen that speckle reduction is best achieved by combining different methods together. One important parameter that needs careful attention is the type of display system. Speckle reduction techniques with DOEs, diffusion films, or screens are useful for area illuminated displays, whereas techniques using sources with reduced coherence length can be used both with area illuminated and flying spot displays. Usage of diffusing materials also causes degradation in the system light efficiency, which is a very important parameter due to power constraints. For example, in the GLV-based display explained above, optical efficiency drops by 15% due to the moving diffuser in the optical train.

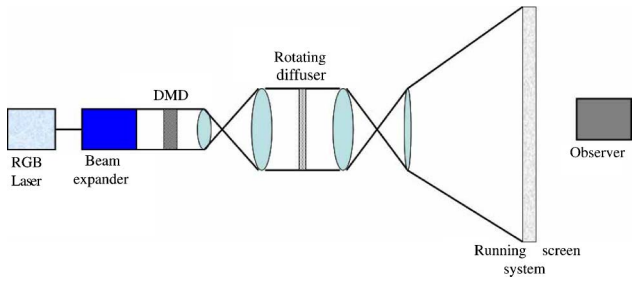

Fig. 13. (Color online) RGB laser rear-projection system design, from Ref. [78].

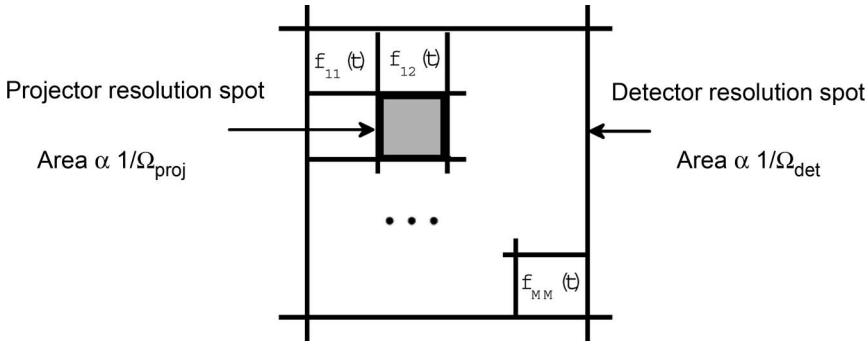

Fig. 14. Division of detector resolution spot into smaller phase cells, from Ref. [80].

Developments of diffusers with low loss will improve the light efficiency of most of the speckle methods discussed so far.

It has been shown that the perceived speckle from backscattered laser light is highly dependent on the characteristics of the projection screen. Riechert *et al.* studied the effect of a quantity termed volume roughness, analogs to the surface roughness, on the depolarization and the path length distributions of the scattered light for various screens and arrived at the conclusion that the speckle contrast can be described by the following equation for a backscattering geometry with a volume scattering screen [81]:

$$C = \left[1 + 2\pi^2 n^2 \left(\frac{\delta\lambda}{\bar{\lambda}}\right)^2 \left(\frac{\sigma_\nu}{\bar{\lambda}}\right)^2\right]^{-\frac{1}{4}}. \quad (4)$$

In Eq. (4), $\delta\lambda$ is the $1/e$ width of the wavelength spectrum of the source, $\bar{\lambda}$ is its mean emission wavelength, n is the refractive index of the volume scatterer, and σ_ν is its volume roughness.

Antispeckle solutions are available commercially. Dyoptyka antispeckle technologies reduce speckle by reducing coherence in the spatial or temporal domains, or both. Dynamic optical components, such as deformable mirrors, are modulated at up to 500 kHz in such a way as to achieve randomized surface shapes. When used with a stationary diffuser, this reduces average spatial coherence. When used with a multimode optical fiber, this reduces average temporal coherence because of the phase delay introduced between higher and lower order modes. In both cases, a very large number of uncorrelated speckle patterns can be created over the observation period.

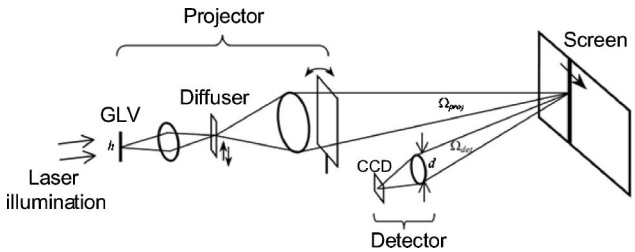

Fig. 15. GLV laser projection system with speckle reduction, from Ref. [80].

6. Optics for Laser Displays

Laser-based displays require special optical components to shape, homogenize, combine, or separate laser beams. The preferred optical components and the coatings on them show variety according to the type, power, and the wavelengths of the lasers used. Although there are overlapping techniques, laser beam shaping can be divided into two categories.

A. Laser Beam Shaping of Single-Emitter Lasers

Beam shaping of single-emitter lasers can be done with reflective and diffractive elements, and the method used mainly depends on the shape and the power of the input beam [82–84].

A simple laser beam shaping technique for single-emitter lasers that uses refractive elements is shown in Fig. 16. It consists of two plano–aspheric lenses in the standard Galilean beam expander configuration. The first lens directs the incident rays so that they are uniformly distributed on the second lens. The second lens collimates the incident beam, the exiting beam propagates almost perfectly collimated, and the optical path length (OPL) is preserved. This configuration allows creation of large collimated beams but requires radially symmetric input beams and works for a certain wavelength. If the wavelengths of the input beam changes, the setup needs adjustment by changing the distance between the two lenses [85]. On the other hand, it is possible to achromatize the two-lens system by using conventional spherical components made of standard glass. Inserting doublets or triplets as external compensators at the exit pupil of the design is a method for color correction [86].

The surface profiles of the above lenses are calculated by ray tracing by considering conservation of

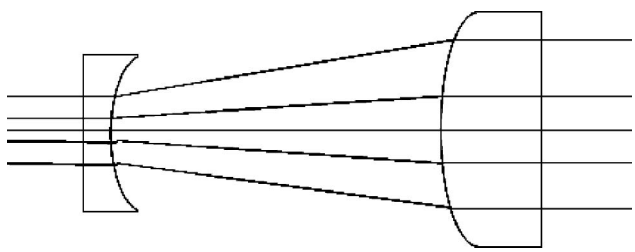

Fig. 16. Beam expander configuration with two plano–aspheric lenses.

energy and OPL conditions. Similar methods are used for transforming an elliptical beam into a Fermi–Dirac output profile by using a two-mirror system [87] and to design gradient-index laser beam shapers [88].

Astigmatism of the beam from an edge-emitting diode laser can be corrected with suitably placed cylindrical lenses with different optical powers [89]. For high-power single-emitter lasers, lens-based shapers may not be suitable, as their performance deteriorates over time [90]. In order to shape a high-power laser beam into a uniform rectangular profile, two external binary phase reflective DOEs can be used. DOEs have a wide variety of applications in display systems, and their properties and different application areas are studied in the literature [91]. Refractive-type DOEs can be used for Gaussian to flat-top conversion of low-power lasers [92], and reflective-type DOEs help handle higher optical powers without experiencing the deterioration problem. If a uniform intensity profile is required at a target plane, a phase element combined with a Fourier transform lens can be used [93]. This configuration requires a Gaussian beam with a uniform phase profile to achieve the required intensity distribution at the target plane.

The methods discussed above use passive optical elements to shape laser beams, which make them sensitive to the input. Another way of shaping a laser beam is using active optical elements such as deformable mirrors, which adjust the spatial phase of the beam before propagating to the target. Improvements in MEMS technology allows fabricating small, fast, high-precision and high-resolution MEMS deformable mirrors using customized surface micromachining [94]. Active elements allow the creation of uniform intensity profiles with different geometries and compensate for nonideal input beams but increase the cost of the system [95,96].

B. Laser Beam Shaping of Multiemitter Lasers

Laser diode arrays are effective sources because of their high power supporting capabilities and lower speckle properties. Delivery of the beam from the array without losing brightness and beam quality is an important task [97]. Different methods for combining the output of laser diode arrays in the spectral and phase domains have been studied in the literature [98–100]. Most of the time, individual emitters in the array have different divergence angles in different axes. A classical method for beam shaping is combining different emitter outputs using a fiber bundle and focusing them into a single fiber. In order to get maximum efficiency, bundle dimensions should be as small as possible, which places restrictions on minimum jacketing and cladding thickness [101]. Design and fabrication of optical fiber couplers for diode arrays have been studied in the literature [102–105], and high-power diode lasers with fiber coupling are commercially available with optical powers up to 200 W [106]. However, if there is a mismatch between the modes of the array emitters and the optical fiber, this approach is not efficient and results in reduced brightness. A prism-based solution for this problem is shown in Fig. 17. In this approach, prism groups divide the beam coming from different emitters along the slow axis and rearrange them along the fast axis [102].

Uniform intensity profiles over an area or along a line from laser diode arrays can be produced using microlens arrays combined with field lenses [107]. The divergence of the emitted rays can be controlled by microlens arrays [108], and the output can be homogenized by combining and mixing the rays from different emitters. Coupling the light efficiently into the microlenses, alignment errors between the emitters and the microlens arrays and fabrication of microlens arrays with precise surface profiles are some of the challenges to be addressed in this approach [109,110], but systems with microlens arrays [111–114] and chirped microlens arrays [115] have been successfully demonstrated.

The most common microlens array configuration for creating uniform illumination is known as the fly's eye configuration, a schematic of which is shown in Fig. 18. It consists of two identical microlens arrays and a field lens. This system will have reduced interference effects if used after a telescope configuration with a rotating random diffuser in between, as shown in Fig. 19 [116,117].

The first array of the above configuration is called the field lens array, and the second array is called the pupil lens array, as it forms the pupil of the system. The combination of two microlens arrays is called a uniformizer or a tandem lens array. The second microlens array is located at the focal plane of the first microlens array, and the level of homogenization is inversely proportional to the pitch of the arrays. A configuration with two identical microlens arrays separated by a focal length can also be used for exit-pupil expansion in display systems and fabrication technologies [118,119]. Alignment methods for those arrays are also given in the literature [120].

An improved design that uses a multiemitter laser and a fly's eye configuration to create a uniform laser line at a plane is shown in Fig. 20 [111,121]. Although designed for a laser printer, this method can be applied to display systems requiring a line

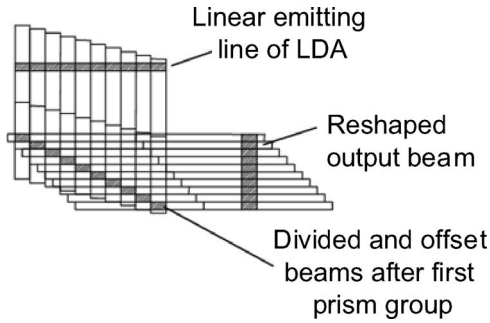

Fig. 17. Side view of the beam-shaping prism groups, from Ref. [102].

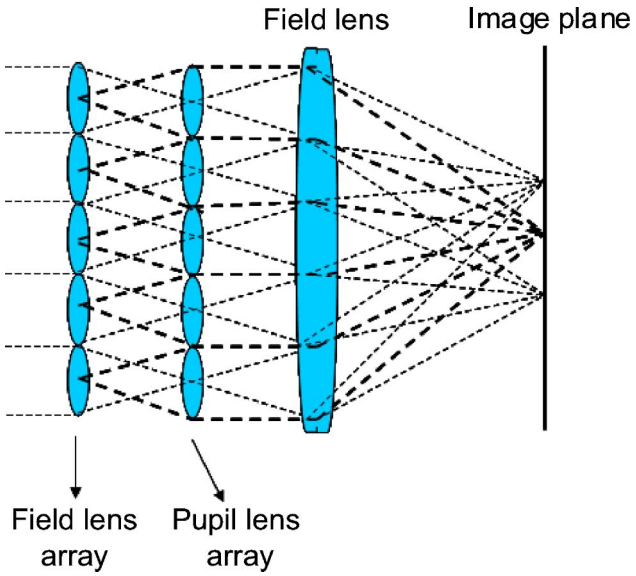

Fig. 18. (Color online) Fly's eye configuration for beam homogenization.

illumination, such as the GLV-based system. In this configuration, beams coming from individual emitters are collimated with the first lenslet array and made to travel through different field lenses and a tandem lens array. The system uses cylindrical microlens arrays to homogenize the laser light only along the line axis and keeps its Gaussian profile along the other axis. As the line is scanned, the intensity along the unhomogenized axis gets averaged. This uniformizer was adapted for a one-dimensional (1D) scanning-based 3D display, which uses array lasers as light sources [121,122]. For full color, an X cube or dichroic mirrors can be used for combining the beams from red, green, and blue lasers [123].

Because of the periodic structure of the microlens arrays, the intensity distribution of the light passing through tandem arrays is divided among the microlenses, which create sharp intensity peaks with equal distances. The performance of tandem arrays can be improved by using asymmetrical or nonperiodic microlens arrays instead of regular arrays. Asymmetrical microlenses allow correction of aberration

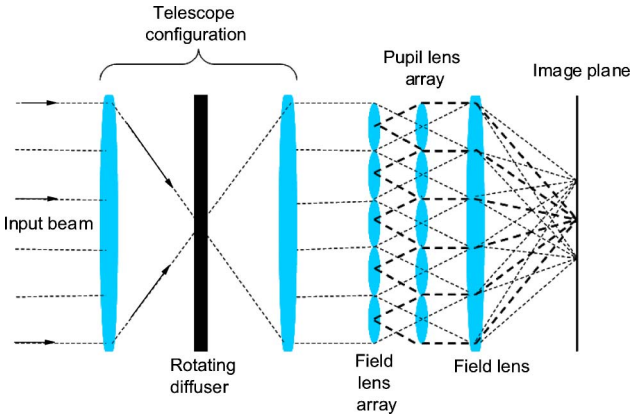

Fig. 19. (Color online) Fly's eye configuration with a diffuser.

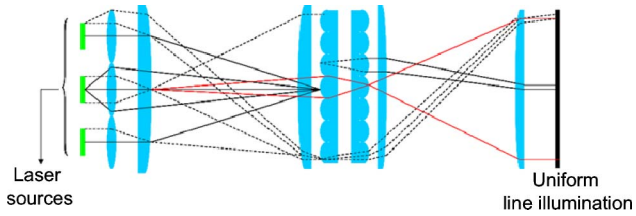

Fig. 20. (Color online) Improved fly's eye configuration for uniform laser line creation from an array of diode lasers.

in off-axis light propagation and eliminate the need for collinear beam alignment by using geometrical adjustment. It is also possible to create homogeneous intensity distributions with desired shapes on a target plane by specifically designing an asymmetric lens array [124].

In chirped microlens arrays, improved homogeneity can be achieved by using nonperiodic arrays with individually shaped lenses, leading to densely located irregular intensity peaks on the target plane [115]. Line generators that can create a uniform line with a thickness of less than 100 μm, from a 1000 W laser diode array have been produced using this approach [125]. Chirped microlens arrays can be fabricated from plane surfaces with a wedge configuration, which enables the use of the reflow of photoresist method. On the other hand, wedge configuration increases the difficulty of the alignment and deflections from the angular surface can cause shifts in the intensity distribution. The output intensity profiles achieved by regular tandem array and chirped tandem array are shown in Fig. 21.

7. Laser Display Systems

Reports of successful implementation of laser-based displays started appearing in the literature in the late 1960s following the first demonstration of the ruby laser in 1960 [1,126,127]. These demonstrations were inspired from the cathode ray tube (CRT), which uses an electron beam to write the image on the screen. After 50 years, advancements in technology provided us with a variety of means by which a laser-based display can be realized each with its own advantages and disadvantages. These systems can

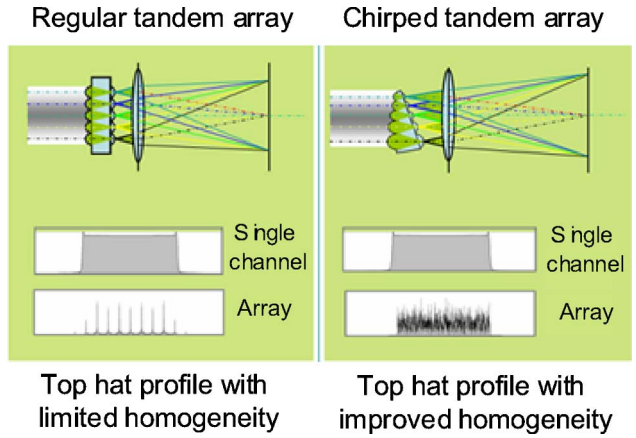

Fig. 21. (Color online) Comparison of intensity patterns of regular and chirped tandem arrays, Ref. [115].

be broadly classified based on the architecture being employed as (i) scanned linear architecture type, which uses a 1D array of pixels [GLV and grating electromechanical system (GEMS)], (ii) scanned beam type [modulation is internal with diode current or external using an electro-optic or acousto-optic modulator (EOM or AOM)], and (iii) two-dimensional (2D) flat panel type [modulation with liquid-crystal display (LCD), digital micromirror device (DMD), or liquid-crystal-on-silicon (LCoS)]. Even though laser-based displays do not have persistence of the pixel similar to the phosphor persistence in CRTs, psychophysical experiments showed that the flicker sensitivity is nearly equal [128]. Thus laser-based displays can replace many other current technologies without adversely affecting user experience. In the following section, successfully demonstrated laser-based display systems are described.

A. Displays with Single-Axis Scanning

Displays following this approach use a 1D array of modulators to form a single column of image, which is then scanned in a direction orthogonal to the length of the line image to form the complete 2D image. This architecture uses microelectromechanical linear array modulators called the GLV by Silicon Light Machines, Incorporated [129], GEMS by Kodak [130] or spatial optical modulator (SOM) by Samsung Electro-Mechanics [131].

All these devices are MEMS, which are fabricated on silicon. The first of these kinds of devices was reported by Solgaard *et al.* in 1992 [132]. GLV and GEMS use electrostatic force to create a grating structure by deflecting tiny reflective ribbons, while SOM utilizes the piezoelectric effect for the same purpose. By controlling the voltage applied to these tiny ribbons, their mechanical shift, and thereby the diffraction of light from the overall grating structure, can be controlled. Figure 22 shows the scanning electron micrograph (SEM) of an actual device from Silicon Light Machines. The moving ribbons of the GLV have no physical contact between each other, and the deflection of the ribbons is only a few hundred nanometers ($\sim\lambda/4$), thereby eliminating mechanical fatigue, wear, and stiction failure modes, which reduce lifetime in MEMS devices.

The ribbons in a GLV device specularly reflect light when they are not actuated. Once actuated, every other ribbon is pulled downward, forming a surface relief grating that diffracts light. As the spacing between the ribbons can be controlled to a very high accuracy using lithographic techniques, the diffraction angle can also be controlled. As illustrated in Fig. 23, the GLV is illuminated with a laser beam that has been formed into a thin line of dimensions comparable to the dimensions of the device. Full-color projection is achieved by using individual GLV devices for red, green, and blue channels or with a single GLV employing color sequential illumination. The full-color output is Fourier transformed, and a spatial filter (Schlieren stop) is used at the

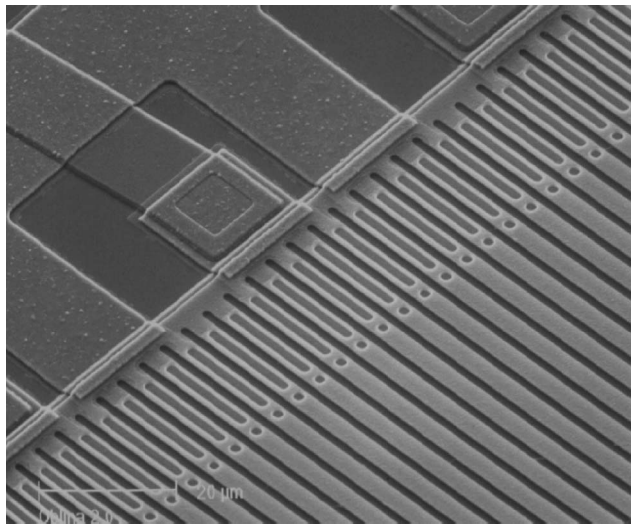

Fig. 22. SEM photograph of GLV ribbons. Photo courtesy of Silicon Light Machines.

Fourier transform plane to filter out either the first orders or the zeroth order. After the order filtering and an inverse Fourier transformation, a scan mirror is used to make a 2D image by horizontally scanning the 1D image. A projection lens system is used for the final projection of the image onto the screen [133]. Figure 23 shows the configuration of a laser projector with GLV devices.

The GLV devices are not polarization sensitive, thereby enabling the use of polarization multiplexing to reduce the speckle contrast to levels below 10%. The contrast achievable with these devices varies from 2000:1 to more than 30,000:1; it was shown that with more device structure, optimizations contrast and lifetime can be increased further [134]. The ribbons in the GLV devices are made of silicon nitride

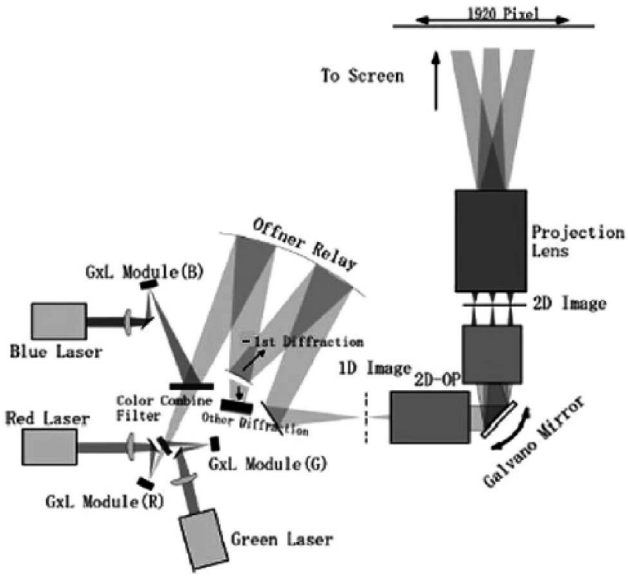

Fig. 23. Schematic of an RGB laser projector with GLV devices. From Ref. [134], Copyright 2007 Society for Information Display.

with a layer of aluminum, and they are capable of handling optical powers of up to $10\,\mathrm{kW/cm^2}$ [135].

Following the success of flat diffraction grating structures, devices with blazed diffraction grating were introduced by Sony [134,136]. These devices are more efficient, owing to the fact that the light is being directed to a single diffraction order, and it produced a contrast ratio that is twice that of the device with a flat grating structure [129]. The Laser Dream Theater at the 2005 World Exposition in Aichi, Japan, employed a 1.09 in. long blazed GLV with 1080 pixels. It used an ultrawide screen, measuring 50 m in length and 10 m in height. The image was produced using 12 GLV projectors giving a brightness of 60,000 lm [134]. Later developments in the technology led to projectors with 1920 pixel horizontal resolution at a frame rate of 240 Hz [137]. Based on GLV technology, the Evans & Sutherland Computer Corporation introduced two commercial projectors. Their ESLP8K-5 model has a resolution of 8192×4096 pixels and 5000 ANSI lumens of brightness with a contrast ratio of 15,000:1.

The SOM and GEMS are also diffractive optical modulators. In the SOM, piezoelectric actuation is used to form the grating profile, while in GEMS, the ribbons are electrostatically made to conform to the substrate features thereby revealing the hidden grating profile [131,138]. All these systems use a similar optical configuration for image formation and projection [131,133,138]. The contrast achievable with these types of 1D modulators is limited by the amplitude mismatch in the light reflected from the passive and active parts of the grating, and careful optimization is required for best performance [131,139,140]. Diffractive modulator technology with a 2D phase grating type light modulator was also reported [141].

Another laser-based display with a similar scanning method is the proposed HELIUM 3D display, which uses single-axis scanning of modulated laser light for forming 3D images by working in conjunction with head trackers. Reflective LCoS microdisplays are used for light modulation in this direct view display [121,122].

The HELIUM 3D display is autostereoscopic, as it sends left and right images of a 3D image to the corresponding eyes of the viewer by forming exit pupils at the location of the eyes of the viewer in a dynamic fashion with the help of head trackers. As shown in the schematic in Fig. 24, the display requires a RGB laser light engine to produce laser line illumination at the modulator plane and a 1D scanner to produce a 2D image. After this image forming section, there is a dynamic spatial light modulator and a special front screen assembly to direct images to the viewing zones with the help of head trackers [122].

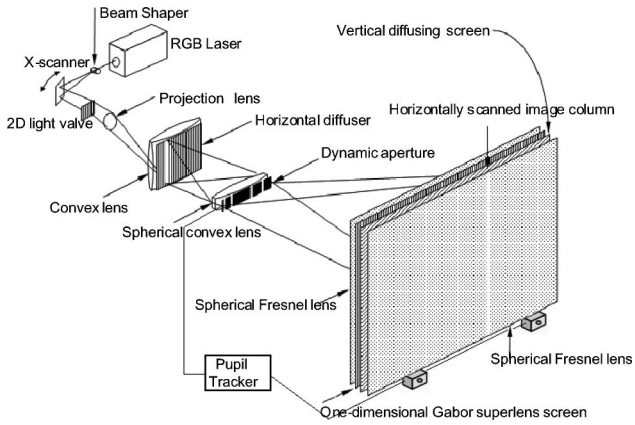

Fig. 24. HELIUM 3D display schematic. Courtesy of HELIUM 3D consortium, which the authors are part of.

B. Displays with Two-Axis Scanning

Most of the earlier laser-based display systems belong to this category [1,126,127]. These types of displays use a slowly converging laser beam, which is modulated by the video signal, to write the images by scanning the beam on the screen using a pair of scanner mirrors. These types of raster scanned displays have the advantage of not requiring a projection lens assembly for image formation. Thus these systems can be very compact and less expensive, making them suitable for the mobile market. Image formation is very similar to that of the electron gun in a CRT. Vertical and horizontal movement of the laser beam is achieved by a two-mirror system in which a very fast polygon mirror scans the horizontal axis while the other mirror slowly scans the vertical axis. The polygon mirror scanner systems were extensively discussed in the literature [142–144]. Developments in MEMS technology has led to the evolution of compact and silent two-axis MEMS scanners that can replace both mirrors mentioned earlier [145]. The raster scanned projection scheme does not require projection lenses, as these systems directly write the image on the screen and the image is always in focus, regardless of the distance of the projection screen or the shape of the projection surface [146]. The schematic of a flying spot laser projector is shown in Fig. 25.

Diode lasers are more suitable for this type of display, as they are directly modulatable by modulating the diode current according to the video signal. Most compact laser projectors use this approach, but other modulator technologies such as AOMs or EOMs can also be used [147,148]. Earlier works in laser-based displays were mainly based on acousto-optic modulation [1,149–151], using acousto-optic devices for both beam modulation and scanning was also discussed in the literature [147]. The laser projection displays reported by Hwang *et al.* used an AOM for beam modulation and a pair of mirrors for scanning. 4 W white light obtained from a krypton–argon laser was used to produce a display with dimensions of $4\,\mathrm{m} \times 3\,\mathrm{m}$ [2,152]. With the introduction of miniature MEMS scanner mirrors, this type of projectors became more compact. The laser television reported by Lee *et al.* used a single-axis MEMS scanner and a polygon mirror for image formation by scanning the screen with a laser beam modulated by AOMs [153]. Further miniaturization of scanner technology led to the

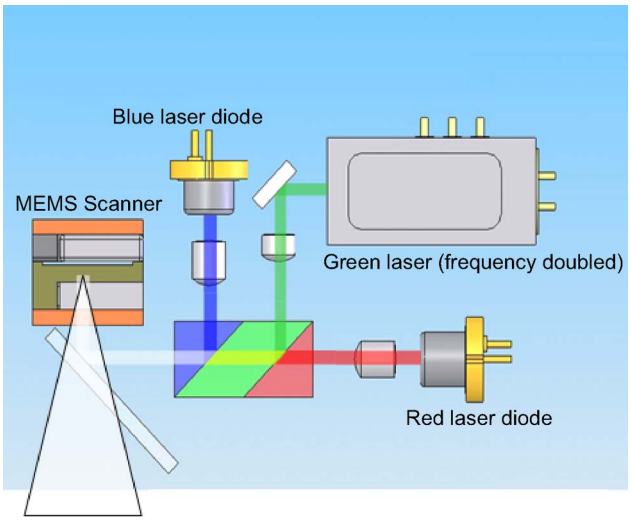

Fig. 25. (Color online) Schematic of a flying spot laser projector. Image courtesy of Microvision, Incorporated.

introduction of a new class of projectors called pico projectors; these use directly modulatable diode lasers and two-axis MEMS scanners, which allow a large reduction in size. Figure 26 shows such a two-axis MEMS device developed by Microvision.

Microvision has demonstrated pico projectors with 2D MEMS scanners and are now preparing for the commercial launch of pico projectors [154]. These pico projectors use diode lasers operating at 442, 532 , and 635 nm as sources. The diode current is modulated based on the video signal and sent to a MEMS scanner after combining the beams.

C. Displays with Direct Two-Dimensional Modulation

Direct modulation of the laser light with 2D modulators such as the DMD from Texas Instruments or LCDs has the advantage of requiring lower beam quality from the laser. As the étendue of these modulators is high, the beam can be many times diffraction limited with no adverse effects on efficiency [3]. Zheng *et al.* demonstrated a projector based on this type of architecture. They used DMD devices for modulating the light [155]. The optical configuration of the projection system can be seen in Fig. 27.

For these types of backlit displays, the required laser beam quality (étendue) depends on the aperture size of the modulator and its angular acceptance [3]. As the étendue of the modulator is higher than the laser beam in most cases, inefficiencies do not arise. There are laser projectors based on reflective and transmissive liquid-crystal (LC) technologies. Mitsubishi introduced LaserVue, a laser-based television in 2008 [156]. This class 1 laser display uses DMD units for light modulation.

The projector reported by Xu *et al.* used transmissive LC microdisplays for modulating the laser light. This projector, which could produce an image with a resolution of 1024×768 pixels on a 60 in. screen, used more than 4 W of white light obtained by red (671 nm), green (532 nm), and blue (473 nm) lasers. Each primary color was modulated separately using individual LC microdisplays [157]. This projector made use of many nonlinear optical conversion processing stages for producing the required primaries. The projector introduced by the company Explay uses reflective LCoS microdisplays. The microprojector from Alcatel-Lucent uses a single reflective LCoS unit, with color sequential illumination by employing a modulation frequency of 180 Hz, divided among the three primaries, which results in a 60 Hz full-color image. This projector uses 635 nm, 532 nm, and 450 nm lasers to produce a 10 lm output with only 1.5 W of electrical power consumption [158].

D. Holographic Laser Projector

The laser projection display by LBO is based on 2D diffraction from diffraction patterns displayed on a microdisplay. The diffraction patterns corresponding to each frame in the video are computed using a proprietary algorithm [159]. The image is converted to a phase only hologram $h_{uv} = \exp j\varphi_{uv}$ and sent to a ferroelectric LC-based microdisplay. The advantage of dropping the amplitude components from the inverse

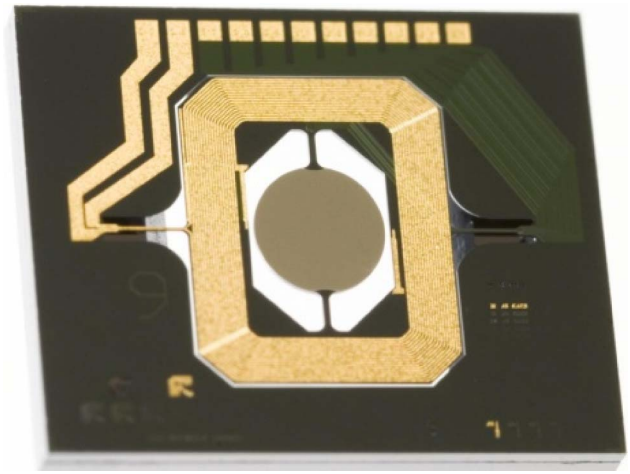

Fig. 26. (Color online) 2D MEMS Scanner from Microvision, Incorporated, Ref. [154].

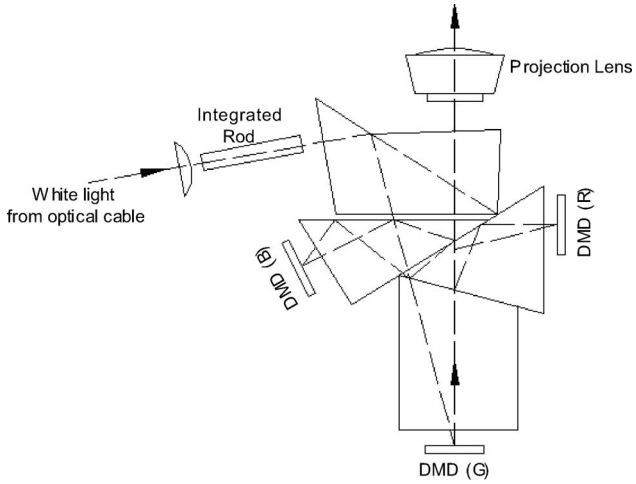

Fig. 27. Schematic of a DMD-based laser projector. Taken from Ref. [155].

Fourier transform of the desired image is that the efficiency is not reduced due to amplitude modulation. As a result, there is no intensity loss due to the modulation optics, and by the process of diffraction the light is directed to brighter areas of the image instead of getting blocked, as in conventional 2D modulator-based displays. As the modulator requires gray scale representation, the projected image bears quantization noise, to minimize this, N number of statistically independent subimages are sent to the microdisplay within the 40 ms response time frame of the eye. This method has the added advantage that, due to the creation of N independent subpatterns, there are N independent speckle patterns leading to a reduction in speckle contrast by $1/\sqrt{N}$. One of the notable advantages is that the wavefront aberrations introduced by the projection optics can be corrected while calculating the diffraction patterns. This means that one can easily assemble a projection system with low-cost optics and then compensate for any wavefront imperfections caused by the optics by incorporating correction factors while calculating the diffraction pattern [160].

The displays from LBO are called holographic because they employ light diffraction in the display but these are not truly holographic and form only a 2D image. Holographic video displays, which can indeed display 3D images, have also been under active development over the last two decades but are currently limited by the capabilities of the available modulation and computation technologies [161]. The Mark I, II, and III series of displays from the Massachusetts Institute of Technology are examples of this type of display [162].

E. Other Laser-Based Displays

Other display types that successfully exploited the positive aspects of laser light are head-mounted displays. These systems were bulky and heavy, but with the incorporation of new technologies they are finding places in medical, automotive, and military applications [163,164]. These types of wearable displays can be seen through, as well, providing real-world images superimposed with information from external sources. These types of displays have been successfully demonstrated [163,165]. A stereoscopic wearable display has been demonstrated by incorporating a deformable membrane mirror to provide focus cues by Schowengerdt *et al.* [166]. It can be presumed that many 3D display technologies [167] will also find laser sources beneficial soon.

8. Summary

Laser-based display technology is undergoing a revolutionary phase change with the introduction of new modulator technologies, MEMS scanners, and efficient as well as low-cost laser sources. In the coming years many of the current displays may be replaced with laser backlit or laser flying spot type displays and projectors. Factors that contributed to the recent developments include new modulation technologies, low-cost and compact diode laser sources, techniques for speckle reduction, and the demand for mobile devices with a large screen.

Direct writing laser projectors require lasers with high beam quality. The OPSL technology might be able to provide high-power beams with high beam quality. Scalability of this technology might extend its range to laser units with a small form factor and high power in the near future. Different speckle reduction methods are available in the literature, with techniques ranging from vibrating screens to multiple sources. Beam shaping is also an important consideration as effective use of available optical power requires carefully designed and optimized optics that fulfill the requirement of the display architecture. Different micromechanical light modulator and scanning technologies have been reported in the literature, which eventually led to successful laser-based displays. Developments in this field are very promising, with size and complexity going down and brightness and resolution going up.

The authors thank the financial support of the European Commission within FP7 under grant 215280 HELIUM 3D project. Help from Karl Byrund and Mark Freeman from Microvision, Incorporated, is gratefully acknowledged. Hakan Urey acknowledges the support from a TUBA-GEBIP award.

References

1. A. Korpel, R. Adler, P. Desmares, and W. Watson, "A television display using acoustic deflection and modulation of coherent light," Appl. Opt. **5**, 1667–1675 (1966).
2. Y. Kim, H. W. Lee, S. Cha, J.-H. Lee, Y. Park, J. Park, S. S. Hong, and Y. M. Hwang, "Full color laser projection display using Kr-Ar laser (white laser) beam-scanning technology," Proc. SPIE **3131**, 2–10 (1997).
3. D. E. Hargis, R. Bergstedt, A. M. Earman, P. Gullicksen, R. Hurtado, A. P. Minich, S. E. Nelte, D. P. Ornelas, M. A. Pessot, E. B. Takeuchi, B. D. Vivian, and J. H. Zarrabi, "Diode-pumped microlasers for display applications," Proc. SPIE **3285**, 115–125 (1998).
4. M. Scholles, K. Frommhagen, C. Gerwig, J. Knobbe, H. Lakner, D. Schlebusch, M. Schwarzenberg, and U. Vogel, "Recent advancements in system design for miniaturized MEMS-based laser projectors," Proc. SPIE **6911**, 69110U (2008).
5. C. Deter and J. Kraenert, "High-resolution scanning laser projection display with diode-pumped solid state lasers," Proc. SPIE **3954**, 175–184 (2000).
6. R. N. Hall, G. E. Fenner, J. D. Kingsley, T. J. Soltys, and R. O. Carlson, "Coherent light emission from GaAs junctions," Phys. Rev. Lett. **9**, 366–368 (1962).
7. M. I. Nathan, W. P. Dumke, G. Burns, F. H. Dill, Jr., and G. Lasher, "Stimulated emission of radiation from GaAs *p-n* junctions," Appl. Phys. Lett. **1**, 62–64 (1962).
8. T. M. Quist, R. H. Rediker, R. J. Keyes, W. E. Krag, B. Lax, A. L. McWhorter, and H. J. Zeigler, "Semiconductor maser of GaAs," Appl. Phys. Lett. **1**, 91–92 (1962).
9. Zh. I. Alferov, V. M. Andreev, E. L. Portnoi, and M. K. Trukan, "AlAs-GaAs heterojunction injection lasers with a low room-temperature threshold," Fiz. Tekh. Poluprovodn. **3**, 1328–1332 (1969).
10. I. Hayashi, M. B. Panish, P. W. Foy, and S. Sumski, "Junction lasers which operate continuously at room temperature," Appl. Phys. Lett. **17**, 109–111 (1970).

11. Y. Suematsu and K. Iga, "Semiconductor lasers in photonics," J. Lightwave Technol. **26**, 1132–1144 (2008).
12. Y. Hirano, S. Yamamoto, Y. Akino, A. Nakamura, T. Yagi, H. Sugiura, and T. Yanagisawa, "High performance micro green laser for laser TV," in *Advanced Solid-State Photonics* (Optical Society of America, 2009), paper WE1.
13. P. Janssens and K. Malfait, "Future prospects of high-end laser projectors," Proc. SPIE **7232**, 72320Y (2009).
14. K. Du, M. Baumann, B. Ehlers, H. G. Treusch, and P. Loosen, "Fiber-coupling technique with micro step-mirrors for high-power diode laser bars," in *Advanced Solid State Lasers*, C. Pollock and W. Bosenberg, eds. (Optical Society of America, 1997), Vol. 10.
15. J. Wang, Z. Yuan, L. Kang, K. Yang, Y. Zhang, and X. Liu, "Study of the mechanism of "smile" in high power diode laser arrays and strategies in improving near-field linearity," in *IEEE 59th Electronic Components and Technology Conference* (IEEE, 2009), pp. 837–842.
16. R. McBride, H. Baker, J.-L. Neron, S. Doric, C. Mariottini, E. Nava, E. Stucchi, and P. Milanesi, "A high-brightness QCW pump source using a pre-aligned GRIN lens array with refractive beam correction," Proc. SPIE **6876**, 687602 (2008).
17. J. W. Goodman, "Some fundamental properties of speckle," J. Opt. Soc. Am **66**, 1145–1150 (1976).
18. J. Endriz, M. Vakili, G. Browder, M. De Vito, J. Haden, G. Harnagel, W. Plano, M. Sakamoto, D. Welch, S. Willing, D. Worland, and H. Yao, "High power diode laser arrays," IEEE J. Quantum Electron. **28**, 952–965 (1992).
19. G. Hollemann, B. Braun, F. Dorsch, P. Hennig, P. Heist, U. Krause, U. Kutschki, and H. Voelckel, "RGB lasers for laser projection displays," Proc. SPIE **3954**, 140–151 (2000).
20. A. Nebel and R. E. Wallenstein, "Concepts and performance of solid state RGB laser sources for large-frame laser projection displays," Proc. SPIE **3954**, 163–166 (2000).
21. J. Gollier, M. H. Hu, D. Ricketts, D. Loeber, V. Bhatia, and D. Pikula, "Multimode DBR laser operation for frequency doubled green lasers in projection displays," in *SID Symposium Digest of Technical Papers* (Society for Information Display, 2008), Vol. 39, pp. 2081–2083.
22. V. Bhatia, S. J. Gregorski, D. Pikula, S. C. Chaparala, D. A. S. Loeber, J. Gollier, Y. Ozeki, Y. Hata, K. Shibatani, F. Nagai, Y. Nakabayashi, N. Mitsugi, and S. Nakano, "63.2: Efficient and compact green laser incorporating adaptive optics for wide operating temperature range," in *SID Symposium Digest of Technical Papers* (Society for Information Display, 2008), Vol. 39, pp. 962–965.
23. J. Capmany, "Simultaneous generation of red, green, and blue continuous-wave laser radiation in Nd^{3+}-doped aperiodically poled lithium niobate," Appl. Phys. Lett. **78**, 144–146 (2001).
24. Z. D. Gao, S. N. Zhu, S.-Y. Tu, and A. H. Kung, "Monolithic red-green-blue laser light source based on cascaded wavelength conversion in periodically poled stoichiometric lithium tantalate," Appl. Phys. Lett. **89**, 181101 (2006).
25. F. L. Williams, D. F. Elkins, J. P. Anderegg, B. D. Winkler, R. R. Christensen, C. C. Farmer, and C. L. Simmons, "Multiwatt high-efficiency CW single-mode visible lasers for ultrahigh-resolution displays," in *Conference on Lasers and Electro-Optics/International Quantum Electronics Conference* (Optical Society of America, 2009), paper PThA2.
26. H. Soda, K.-I. Iga, C. Kitahara, and Y. Suematsu, "GaInAsP/InP surface emitting injection lasers," Jpn. J. Appl. Phys. **18**, 2329–2330 (1979).
27. J. V. Michael Bove and W. Sierra, "P-125: Personal projection, or how to put a large screen in a small device," in *SID Symposium Digest of Technical Papers* (Society for Information Display, 2003), Vol. 34, pp. 708–711.
28. G. Duggan, D. A. Barrow, T. Calvert, M. Maute, V. Hung, B. McGarvey, J. D. Lambkin, and T. Wipiejewski, "Red vertical cavity surface emitting lasers (VCSELs) for consumer applications," Proc. SPIE **6908**, 69080G (2008).
29. S. Hallstein, G. P. Carey, R. Carico, R. Dato, J. J. Dudley, A. M. Earman, M. J. Finander, G. Giaretta, J. Green, H. J. Hofler, F. Hu, M. Jansen, C. P. Kocat, S. Lim, J. Krueger, A. Mooradian, G. Niven, Y. Okuno, F. G. Patterson, A. Tandon, and A. Umbrasas, "RGB laser light sources for projection displays," in *2007 IEEE LEOS Annual Meeting Conference Proceedings, Vols. 1 and 2* (IEEE, 2007), pp. 254–255.
30. M. Dawson, J. E. Hastie, S. Calvez, N. Laurand, D. Burns, and A. J. Kemp, "Semiconductor disk lasers: recent developments in bulk and micro-lasers," in *Advanced Solid-State Photonics* (Optical Society of America, 2009), paper ME1.
31. S. Lutgen, T. Albrecht, P. Brick, W. Reill, J. Luft, and W. Späth, "8 W high-efficiency continuous-wave semiconductor disk laser at 1000 nm," Appl. Phys. Lett. **82**, 3620–3622 (2003).
32. G. B. Kim, J.-Y. Kim, J. Lee, J. Yoo, K.-S. Kim, S.-M. Lee, S. Cho, S.-J. Lim, T. Kim, and Y. Park, "End-pumped green and blue vertical external cavity surface emitting laser devices," Appl. Phys. Lett. **89**, 181106 (2006).
33. U. Steegmuller, M. Kuhnelt, H. Unold, T. Schwarz, R. Schulz, S. Illek, I. Pietzonka, H. Lindberg, M. Schmitt, and U. Strauss, "Green laser modules to fit laser projection out of your pocket," Proc. SPIE **6871**, 687117 (2008).
34. U. Steegmueller, M. Kuehnelt, H. Unold, T. Schwarz, R. Schulz, and F. Singer, "Late-news paper: RGB laser for mobile projection devices," in *SID Symposium Digest of Technical Papers* (Society for Information Display, 2007), Vol. 38, pp. 16–18.
35. S. Calvez, J. Hastie, M. Guina, O. Okhotnikov, and M. Dawson, "Semiconductor disk lasers for the generation of visible and ultraviolet radiation," Laser Photon. Rev. **3**, 407–434 (2009).
36. A. C. Tropper, H. D. Foreman, A. Garnache, K. G. Wilcox, and S. H. Hoogland, "Vertical-external-cavity semiconductor lasers," J. Phys. D **37**, 75–85 (2004).
37. J. D. Mollon, "The origins of modern color science," in *The Science of Color*, 2nd ed., S. K. Shevell, ed. (Elsevier, 2003).
38. Y.-C. Ko, J.-W. Cho, Y.-K. Mun, H.-G. Jeong, W.-K. Choi, J.-H. Lee, J.-W. Kim, J.-B. Yoo, and J.-H. Lee, "Eye-type scanning mirror with dual vertical combs for laser display," Proc. SPIE **5721**, 14–22 (2005).
39. Y.-C. Ko, J.-W. Cho, Y.-K. Mun, H.-G. Jeong, W. K. Choi, J.-W. Kim, Y.-H. Park, J.-B. Yoo, and J.-H. Lee, "Eye-type scanning mirror with dual vertical combs for laser display," Sens. Actuators A, Phys. **126**, 218–226 (2006).
40. M. Ebner, "Color reproduction," in *Color Constancy* (Wiley, 2007).
41. J.-P. Meyn, "Colour mixing based on daylight," Eur. J. Phys. **29**, 1017–1031 (2008).
42. A. D. Broadbent, "A critical review of the development of the CIE1931 RGB color-matching functions," Color Res. Appl. **29**, 267–272 (2004).
43. S. Wen, "Design of relative primary luminances for four-primary displays," Displays **26**, 171–176 (2005).
44. T. Ajito, T. Obi, M. Yamaguchi, and N. Ohyama, "Expanded color gamut reproduced by six-primary projection display," Proc. SPIE **3954**, 130–137 (2000).
45. S. Roth, I. Ben-David, M. Ben-Chorin, D. Eliav, and O. Ben-David, "10.2: wide gamut, high brightness multiple primaries single panel projection displays," in *SID Symposium Digest of Technical Papers* (Society for Information Display, 2003), Vol. 34, pp. 118–121.
46. M. Ou-Yang and S.-W. Huang, "Design considerations between color gamut and brightness for multi-primary color displays," J. Display Technol. **3**, 71–82 (2007).
47. Y. Cheng, X. Liu, and H. Li, "A color temperature adjustment method for multiprimary displays using nonlinear programming," Color Res. Appl. **34**, 201–204 (2009).

48. F. E. Doany, R. N. Singh, A. E. Rosenbluth, and G. L.-T. Chiu, "Projection display throughput: efficiency of optical transmission and light-source collection," IBM J. Res. Dev. **42**, 387–399 (1998).
49. E. H. Stupp and M. S. Brennesholtz, *Projection Displays*, Wiley–SID Series in Display Technology (Wiley, 1998).
50. G. C. de Wit, "Contrast budget of head-mounted displays," Opt. Eng. **41**, 2419–2426 (2002).
51. H. Urey, N. Nestorovic, B. Ng, and A. Gross, "Optics designs and system MTF for laser scanning displays," Proc. SPIE **3689**, 238–248 (1999).
52. M. H. Niemz, "Laser-tissue interactions fundamentals and applications," in *Biological and Medical Physics, Biomedical Engineering*, 3rd ed. (Springer , 2003).
53. D. H. Sliney, J. Mellerio, V.-P. Gabel, and K. Schulmeister, "What is the meaning of threshold in laser injury experiments? Implications for human exposure limits," Health Phys. **82**, 335–347 (2002).
54. M. A. Mainster, "Blinded by the light—not!," Arch. Ophthalmol. **117**, 1547–1548 (1999).
55. M. A. Mainster, B. E. Stuck, and J. Brown, "Assessment of alleged retinal laser injuries," Arch. Ophthalmol. **122**, 1210–1217 (2004).
56. International Commission on Non-Ionizing Radiation Protection, "Revision of guidelines on limits of exposure to laser radiation of wavelengths between 400 nm and 1.4 μm," Health Phys. **79**, 431–440 (2000).
57. D. A. Corder, J. B. O'Hagan, and J. R. Tyrer, "Safety assessments of visible scanned laser beams," J. Radiol. Prot. **17**, 231–238 (1997).
58. J. A. Agostinelli, "Laser projector having silhouette blanking for objects in the output light path," U.S. patent 6,984,039 (10 January 2006).
59. R. Henderson and K. Schulmeister, *Laser Safety* (Taylor & Francis, 2004).
60. K. Bylund, D. H. Sliney, and M. Beard, "Comparative evaluation of ocular hazards from projectors—laser and lamp projectors," in *International Laser Safety Conference (ILSC) 2009* (Laser Institute of America, 2009), paper 1304.
61. H.-D. Reidenbach, "Laser Safety," *Springer Handbook of Lasers and Optics*, 1st ed. (Springer Science+Business Media, 2007).
62. G. D. Costa and J. Ferrari, "Anisotropic speckle patterns in the light scattered by rough cylindrical surfaces," Appl. Opt. **36**, 5231–5237 (1997).
63. B. B. Gorbatenko, V. P. Ryabukho, and L. A. Maksimova, "Reconstructing an object image using the laser speckle pattern of the diffraction field," Tech. Phys. Lett. **30**, 741–743 (2004).
64. D. Yu, M. Stern, and J. Katz, "Speckle noise in laser bar-code-scanner systems," Appl. Opt. **35**, 3687–3694 (1996).
65. L. Wang, T. Tschudi, T. Halldórsson, and P. R. Pétursson, "Speckle reduction in laser projection systems by diffractive optical elements," Appl. Opt. **37**, 1770–1775 (1998).
66. W. Liu and C. Zhou, "Femtosecond laser speckles," Appl. Opt. **44**, 6506–6510 (2005).
67. J. C. Dainty, "Stellar speckle interferometry," in *Laser Speckle and Related Phenomena* (Springer-Verlag, 1975).
68. F. Riechert, F. Glöckler, and U. Lemmer, "Method to determine the speckle characteristics of front projection screens," Appl. Opt. **48**, 1316–1321 (2009).
69. T. W. Ng, "Optical distance sensing using digital speckle shearing interferometry," Opt. Lasers Eng. **26**, 449–460 (1997).
70. T. W. Ng, "The optical mouse as a two-dimensional displacement sensor," Sens. Actuators A, Phys. **107**, 21–25 (2003).
71. J. D. Briers, "Laser speckle contrast imaging for measuring blood flow," Opt. Appl. **37**, 139–152 (2007).
72. T. Iwai and T. Asakura, "Speckle reduction in coherent information processing," Proc. IEEE **84**, 765–781 (1996).
73. I. Peled, M. Zenou, B. Greenberg, and Z. Kotler, "MEMS based speckle reduction obtained by angle diversity for fast imaging," in *Conference on Lasers and Electro-Optics/International Quantum Electronics Conference,* OSA Technical Digest (CD) (Optical Society of America, 2009), paper JTuD44.
74. A. Furukawa, N. Ohse, Y. Sato, D. Imanishi, K. Wakabayashi, S. Ito, K. Tamamura, and S. Hirata, "Effective speckle reduction in laser projection displays," Proc. SPIE **6911**, 69110T (2008).
75. F. Riechert, G. Bastian, and U. Lemmer, "Laser speckle reduction via colloidal-dispersion-filled projection screens," Appl. Opt. **48**, 3742–3749 (2009).
76. M. N. Akram, V. Kartashov, K. Wang, G. Ouyang, and X. Chen, "Laser speckle reduction using a dynamic polymer-based diffraction grating spatial phase modulator," Proc. SPIE **7382**, 73822H (2009).
77. H. Urey, "Diffractive exit-pupil expander for display applications," Appl. Opt. **40**, 5840–5851 (2001).
78. S. C. Shin, S. S. Yoo, S. Y. Lee, C.-Y. Park, S.-Y. Park, J. W. Kwon, and S.-G. Lee, "Removal of hot spot speckle on rear projection screen using the rotating screen system," J. Display Technol. **2**, 79–84 (2006).
79. F. Riechert, G. Craggs, Y. Meuret, B. V. Giel, H. Thienpont, U. Lemmer, and G. Verschaffelt, "Low-speckle laser projection with a broad-area vertical-cavity surface-emitting laser in the nonmodal emission regime," Appl. Opt. **48**, 792–798 (2009).
80. J. I. Trisnadi, "Speckle contrast reduction in laser projection displays," Proc. SPIE **4657**, 131–137 (2002).
81. F. Riechert, F. Glöckler, and U. Lemmer, "Method to determine the speckle characteristics of front projection screens," Appl. Opt. **48**, 1316–1321 (2009).
82. D. L. Shealy, "Historical perspective of laser beam shaping," Proc. SPIE **4770**, 28–47 (2002).
83. F. M. Dickey, L. S. Weichman, and R. N. Shagam, "Laser beam shaping techniques," Proc. SPIE **4065**, 338–348 (2000).
84. P. Nussbaum and H. P. Herzig, "Refractive and diffractive elements for micro-optical systems," Proc. SPIE **3226**, 32–43 (1997).
85. W. Jiang and D. L. Shealy, "Development and testing of a refractive laser beam shaping system," Proc. SPIE **4095**, 165–175 (2000).
86. C. M. Jefferson and J. A. Hoffnagle, "An achromatic refractive laser beam reshaper," Proc. SPIE **5175**, 1–11 (2003).
87. D. L. Shealy and S.-H. Chao, "Geometric optics-based design of laser beam shapers," Opt. Eng. **42**, 3123–3138 (2003).
88. D. L. Shealy and S.-H. Chao, "Design of GRIN laser beam shaping system," Proc. SPIE **5525**, 138–147 (2004).
89. S. Jutamulia, H. Zhai, and G. Mu, "Beam correction optics for laser diodes," Proc. SPIE **6024**, 60240I (2006).
90. S. N. Toma, A. Alexandrescu, D. Apostol, V. Nascov, and D. Cojoc, "Gaussian to rectangular laser beam shaping using diffractive optical elements," Proc. SPIE **5972**, 59721G (2005).
91. G. M. Morris, D. H. Raguin, M. Rossi, and P. M. Emmel, "Diffractive optics technology for projection displays," Proc. SPIE **2650**, 112–119 (1996).
92. F. Li, Z. Lu, H. Li, and J. Liao, "Nearly diffraction-limited size flat-top laser beam shaper," Proc. SPIE **4095**, 189–195 (2000).
93. S. C. Holswade and F. M. Dickey, "Gaussian laser beam shaping: test and evaluation," Proc. SPIE **2863**, 237–245 (1996).
94. S. Menn, S. A. Cornelissen, and P. A. Bierden, "Advances in MEMS deformable mirror technology for laser beam shaping," Proc. SPIE **6663**, 66630M (2007).
95. S. Avino, B. Potsaid, and J. T. Wen, "Super-Gaussian laser beam shaping using deformable mirrors and intrinsic beam quality metrics," Proc. SPIE **7266**, 72660P (2008).
96. B. G. Henderson and J. D. Mansell, "Laser beam shaping with membrane deformable mirrors," Proc. SPIE **7093**, 70930I (2008).

97. T. Fan, "Laser beam combining for high-power, high-radiance sources," IEEE J. Sel. Top. Quantum Electron. **11**, 567–577 (2005).
98. T. Y. Fan and A. Sanchez, "Coherent (phased array) and wavelength (spectral) beam combining compared (invited paper)," Proc. SPIE **5709**, 157–164 (2005).
99. S. C. Tidwell, S. Roman, D. Jander, and D. D. Lowenthal, "Spectral beam combining of diode laser bars achieve efficient near diffraction limited output power," Proc. SPIE **4973**, 42–46 (2003).
100. E. J. Bochove, "Spectral beam combining of fiber lasers: tolerances, lens design, and microlens array inclusion," Proc. SPIE **4629**, 31–38 (2002).
101. B. J. Skutnik and H. Park, "Fiber coupling of laser diode arrays for high brightness: cladding considerations," Proc. SPIE **4629**, 86–93 (2002).
102. P. Y. Wang, A. Gheen, and Z. Wang, "Beam shaping technology for laser diode arrays," Proc. SPIE **4770**, 131–135 (2002).
103. L. Li, "Coupling of high-power diode laser arrays and fibers," Proc. SPIE **4225**, 201–203 (2000).
104. C. Zhou, Y. Liu, W. Xie, and C. Du, "Analysis and design of fiber-coupled high-power laser diode array," Proc. SPIE **5177**, 140–145 (2003).
105. N. P. Ostrom, M. Gall, and B. O. Faircloth, "Development of high power high brightness fiber coupled diode laser systems," Proc. SPIE **6104**, 61040N (2006).
106. S. Heinemann, B. Regaard, T. Schmidt, and B. Lewis, "High-brightness fiber-coupled single emitter arrays," Proc. SPIE **7198**, 71980Q (2009).
107. T. R. M. Sales, "Structured microlens arrays for beam shaping," Opt. Eng. **42**, 3084–3085 (2003).
108. Q. Deng, C. Du, C. Wang, C. Zhou, X. Dong, Y. Liu, and T. Zhou, "Microlens array for stacked laser diode beam collimation," Proc. SPIE **5636**, 666–670 (2005).
109. Q. Tang, "Refractive microlens array integration with linear high-power semiconductor laser array," Proc. SPIE **3879**, 176–180 (1999).
110. X. Jiang and D. Liu, "The main factors which affect coupling efficiency of high-power semiconductor laser array and selfoc lens array," Proc. SPIE **6823**, 682308 (2007).
111. A. F. Kurtz, "Design of a laser printer using a laser array and beam homogenizer," Proc. SPIE **4095**, 147–153 (2000).
112. E. T. Kana, S. Bollanti, P. D. Lazzaro, and D. Murra, "Beam homogenization: theory, modeling, and application to an excimer laser beam," Proc. SPIE **5777**, 716–724 (2005).
113. A. Tuantranont, V. M. Bright, W. Zhang, J. Zhang, and Y. C. Lee, "Self-aligned assembly of microlens arrays with micromirrors," Proc. SPIE **3878**, 90–100 (1999).
114. B. V. Giel, Y. Meuret, and H. Thienpont, "Using a fly's eye integrator in efficient illumination engines with multiple light-emitting diode light sources," Opt. Eng. **46**, 043001 (2007).
115. F. C. Wippermann, P. Dannberg, A. Bräuer, and S. Sinzinger, "Improved homogenization of fly's eye condenser setups under coherent illumination using chirped microlens arrays," Proc. SPIE **6466**, 64660R (2007).
116. M. Zimmermann, N. Lindlein, R. Voelkel, and K. J. Weible, "Microlens laser beam homogenizer: from theory to application," Proc. SPIE **6663**, 666302 (2007).
117. T. Zuo, T. Chen, and C. Li, "Design of fly's eye homogenizer for excimer laser micromachining," Proc. SPIE **4223**, 40–44 (2000).
118. A. Akatay, A. Waddie, H. Suyal, M. Taghizadeh, and H. Urey, "Comparative performance analysis of 100% fill-factor microlens arrays fabricated by various methods," Proc. SPIE **6185**, 61850C (2006).
119. C. Du, B. Chen, C. Qiu, L. Bai, Q. Deng, C. Zhou, and L. Zhou, "Microlens array and application systems," Proc. SPIE **4231**, 153–157 (2000).
120. H. Urey and K. D. Powell, "Microlens-array-based exit-pupil expander for full-color displays," Appl. Opt. **44**, 4930–4936 (2005).
121. E. Erden, V. C. Kishore, H. Ürey, H. Baghsiahi, E. Willman, S. E. Day, D. R. Selviah, F. A. Fernandez, and P. Surman, "Laser scanning based autostereoscopic 3D display with pupil tracking," in *LEOS Annual Meeting Conference Proceedings,* (IEEE, 2009), pp. 10–11.
122. V. C. Kishore, E. Erden, H. Urey, H. Baghsiahi, E. Willman, S. E. Day, D. R. Selviah, F. Aníbal Fernández, and P. Surman, "Laser scanning 3D display with dynamic exit pupil," in *Proceedings of the 29th International Display Research Conference* (Society for Information Display, 2009), pp. 492–495.
123. J. Popelek and Y. Li, "X-cube: an eight-port beamsplitting device," Proc. SPIE **4114**, 122–128 (2000).
124. O. Homburg, A. Bayer, T. Mitra, J. Meinschien, and L. Aschke, "Beam shaping of high power diode lasers benefits from asymmetrical refractive micro-lens arrays," Proc. SPIE **6876**, 68760B (2008).
125. A. Bayer, J. Meinschien, T. Mitra, and M. Brodner, "Beam shaping of line generators based on high power diode lasers to achieve high intensity and uniformity levels," Proc. SPIE **7062**, 70620X (2008).
126. T. H. Maiman, "Stimulated optical radiation in ruby," Nature **187**, 493–494 (1960).
127. C. E. Baker, "Laser display technology," IEEE Spectrum **5**, 39–50 (1968).
128. J. P. Kelly, S. Turner, H. L. Pryor, E. S. Viirre, E. J. Seibelb, and T. A. Furness, III, "Vision with a scanning laser display: comparison of flicker sensitivity to a CRT," Displays **22**, 169–175 (2001).
129. N. Eguchi, "GxL Laser Dream Theater at the Aichi Expo (equivalent to 2005 inch TV)," in *IDW '06: Proceedings of the 13th International Display Workshops, Vols. 1–3* (2006), pp. 9–12.
130. M. W. Kowarz, J. C. Brazas, and J. G. Phalen, "Conformal grating electromechanical system (GEMS) for high-speed digital light modulation," in *The Fifteenth IEEE International Conference On Micro Electro Mechanical Systems* (IEEE, 2002), pp. 568–573.
131. S. K.Yun, "Spatial optical modulator (SOM): Samsung's light modulator for next-generation laser displays," J. Soc. Inf. Display **15**, 321–333 (2007).
132. O. Solgaard, F. S. A. Sandejas, and D. M. Bloom, "Deformable grating optical modulator," Opt. Lett. **17**, 688–690 (1992).
133. J. I. Trisnadi, C. B. Carlisle, and R. Monteverde, "Overview and applications of grating-light-valve-based optical write engines for high-speed digital imaging," Proc. SPIE **5348**, 52–64 (2004).
134. H. Tamada, "Invited paper: blazed GxLP™ light modulators for laser projectors," J. Soc. Inf. Disp. **15**, 817–823 (2007).
135. D. T. Amm and R. W. Corrigan, "Optical performance of the Grating Light Valve technology," Proc. SPIE **3634**, 71–78 (1999).
136. X. Li, C. Antoine, D. Lee, J.-S. Wang, and O. Solgaard, "Tunable blazed gratings," J. Microelectromech. Syst. **15**, 597–604 (2006).
137. H. Kikuchi, S. Hashimoto, S. Tajiri, T. Hayashi, Y. Sugawara, M. Oka, Y. Akiyama, A. Nakamura, and N. Eguchi, "56.1: high-frame-rate, high-contrast grating light valve laser projection display," in *SID Symposium Digest of Technical Papers* (Society for Information Display, 2008), Vol. 39, pp. 846–849.
138. J. C. Brazas and M. W. Kowarz, "High-resolution laser-projection display system using a grating electromechanical system (GEMS)," Proc. SPIE **5348**, 65–75 (2004).
139. S. Yun, J. Song, I. Yeo, Y. Choi, V. Yurlov, S. An, H. Park, H. Yang, Y. Lee, K. Han, I. Shyshkin, A. Lapchuk, K. Oh, S. Ryu, J. Jang, C. Park, C. Kim, S. Kim, E. Kim, K. Woo, J. Yang, E.

Kim, J. Kim, S. Byun, S. Lee, O. Lim, J. Cheong, Y. Hwang, G. Byun, J. Kyoung, S. Yoon, J. Lee, T. Lee, S. Hong, Y. Hong, D. Park, J. Kang, W. Shin, S. Lee, S. Oh, B. Song, H. Kim, C. Koh, Y. Ryu, H. Lee, and Y. Baek, "Spatial optical modulator (SOM): high-density diffractive laser projection display," Proc. SPIE **6487**, 648710 (2007).
140. V. Yurlov, A. Lapchuk, S. K. Yun, J. Song, K. Lee, I. Yeo, and S. An, "A study of image contrast restriction in displays using diffractive spatial light modulators," Displays **31**, 15–24 (2010).
141. S. Jiyong, H. Shanglian, Z. Jie, Z. Zhihai, and Z. Yong, "Two-dimensional grating light modulator for projection display," Appl. Opt. **47**, 2813–2820 (2008).
142. G. F. Marshall, G. A. Rynkowski, and M. Ketabchi, "Polygonal scanners for TV and HDTV laser projectors: spatial and temporal tolerances versus resolution," Proc. SPIE **1988**, 223–241 (1993).
143. G. F. Marshall and J. I. Montagu, "Advances in oscillatory optical scanners," Proc. SPIE **2383**, 440 (1995).
144. G. F. Marshall, "Stationary ghost images outside the image format of the scanned field image plane," Proc. SPIE **4773**, 132–140 (2002).
145. A. D. Yalcinkaya, H. Urey, D. Brown, T. Montague, and R. Sprague, "Two-axis electromagnetic microscanner for high resolution displays," J. Microelectromech. Syst. **15**, 786–794 (2006).
146. H.-M. Jeong, Y.-H. Park, Y.-C. Cho, J. Hwang, S.-M. Chang, S.-J. Kang, H.-K. Jeong, J. O. Kim, and J.-H. Lee, "Slow scanning electromagnetic scanner for laser display," J. Micro/Nanolith. MEMS and MOEMS **7**, 043003 (2008).
147. B. S. Gurevich, "Laser projection displays based on acoustooptic devices," J. Opt. Technol. **70**, 500–503 (2003).
148. J. D. Beasley, "Electrooptic laser scanner for TV projection display," Appl. Opt. **10**, 1934–1936 (1971).
149. W. H. Watson and A. Korpel, "Equalization of acoustooptic deflection cells in a laser color TV system," Appl. Opt. **9**, 1176–1179 (1970).
150. A. Fukumoto, M. Kawabuchi, and H. Hayami, "Raster-scanned laser display system using two-dimensional TeO_2 acoustooptic light deflector," Electron. Commun. Jpn. **58**, 115–123 (1975).
151. A. N. Drozhzhin, L. A. Kosovskii, L. N. Mikhailova, and K. I. Chamorovskii, "Laser television display unit," Sov. J. Quantum Electron. **5**, 1287–1288 (1975).
152. Y. M. Hwang, J.-H. Lee, Y. Park, J. Park, S. Cha, and Y. Kim, "200 in. full-color laser projection display," Proc. SPIE **3296**, 116–125 (1998).
153. J.-H. Lee, Y.-K. Mun, S.-W. Do, Y.-C. Ko, D.-H. Kong, B.-S. Choi, J.-M. Kim, C.-W. Hong, and D.-Y. Jeon, "Laser TV for home theater," Proc. SPIE **4657**, 138–145 (2002).
154. Microvision, "http://microvision.com/," (accessed 4 December 2009).
155. G. Zheng, B. Wang, T. Fang, H. Cheng, Y. Qi, Y. W. Wang, B. X. Yan, Y. Bi, Y. Wang, S. W. Chu, T. J. Wu, J. K. Xu, H. T. Min, S. P. Yan, C. W. Ye, and Z. D. Jia, "Laser digital cinema projector," J. Display Technol. **4**, 314–318 (2008).
156. Mitsubishi Electric, "Mitsubishi Digital Electronics America introduces new category of large-format televisions with groundbreaking laser technology," press release of 7 January (Mitsubishi Electric, 2008), pp. 1–2.
157. Z. Xu and Y. Bi, "Large laser projection displays utilizing all-solid-state RGB lasers," Proc. SPIE **5632**, 115–122 (2005).
158. R. Ryf, G. Chen, N. Basavanhally, M. Dinu, A. Duque, Y. L. Low, J. M. Wiesenfeld, Y. Shapiro, and R. Giles, "The Alcatel-Lucent microprojector: what every cell phone needs," Bell Labs Tech. J. **14**, 99–112 (2009).
159. E. Buckley, "70.2: Invited paper: holographic laser projection technology," in *SID Symposium Digest of Technical Papers* (Society for Information Display, 2008), Vol. 39, pp. 1074–1079.
160. E. Buckley, R. Isele, and D. Stindt, "14.2 novel human-machine interface (HMI) design enabled by holographic laser projection," in *SID Symposium Digest of Technical Papers* (Society for Information Display, 2009), pp. 172–177.
161. C. Slinger, C. Cameron, and M. Stanley, "Computer-generated holography as a generic display technology," Computer **38**, 46–53 (2005).
162. Stephen A. Benton and V. M. Bove, Jr., *Holographic Imaging* (Wiley , 2008).
163. K. Keller, A. State, and H. Fuchs, "Head mounted displays for medical use," J. Display Technol. **4**, 468–472 (2008).
164. T. H. Harding, C. E. Rash, and S. J. Dennis, "Evaluation of Microvision SD2500 scanning laser display," Proc. SPIE **6224**, 62240R (2006).
165. O. Cakmakci and J. Rolland, "Head-worn displays: a review," J. Display Technol. **2**, 199–216 (2006).
166. B. T. Schowengerdt, E. J. Seibel, N. L. Silverman, and T. A. Furness III, "Stereoscopic retinal scanning laser display with integrated focus cues for ocular accommodation," Proc. SPIE **5291**, 366–376 (2004).
167. P. Benzie, J. Watson, P. Surman, I. Rakkolainen, K. Hopf, H. Urey, V. Sainov, and C. von Kopylow, "A survey of 3DTV displays: techniques and technologies," IEEE Trans. Circuits Syst. Video Technol. **17**, 1647–1658 (2007).
168. W. S. C. Chang, *Principles of Lasers and Optics* (Cambridge U. Press, 2005).